Bacteriophage λ RexA and RexB Functions Assist the Transition from Lysogeny to Lytic Growth

running title: λ Rex proteins assist phage lytic development

Lynn C. Thomason[1,2], Carl J. Schiltz[3,4], Carolyn Court[2], Christopher J. Hosford[3,5], Myfanwy C. Adams[3], Joshua S. Chappie[3], and Donald L. Court[2]

[1]Basic Science Program, Frederick National Laboratory for Cancer Research, Frederick, MD 21702

[2]RNA Biology Laboratory, National Cancer Institute/Frederick Cancer Research and Development Center, Frederick, MD 21702

[3]Department of Molecular Medicine, Cornell University, Ithaca, NY 14850

[4]Present address: Department of Biological Sciences and Center for Structural Biology, Vanderbilt University, Nashville, TN 37232, USA

[5]Present address: New England Biolabs, Inc., Ipswich, MA, USA

Corresponding author: Lynn Thomason thomasol@mail.nih.gov (301) 846-7206

Summary

The CI and Cro repressors of bacteriophage λ create a bistable switch between lysogenic and lytic growth. In λ lysogens, CI repressor expressed from the P_{RM} promoter blocks expression of the lytic promoters P_L and P_R to allow stable maintenance of the lysogenic state. When lysogens are induced, CI repressor is inactivated and Cro repressor is expressed from the lytic P_R promoter. Cro repressor blocks P_{RM} transcription and CI repressor synthesis to ensure that the lytic state proceeds. RexA and RexB proteins, like CI, are expressed from the P_{RM} promoter in λ lysogens; RexB is also expressed from a second promoter, P_{LIT}, embedded in *rexA*. Here we show that RexA binds CI repressor and assists the transition from lysogenic to lytic growth, using both intact lysogens and defective prophages with reporter genes under control of the lytic P_L and P_R promoters. Once lytic growth begins, if the bistable switch does return to the immune state, RexA expression lessens the probability that it will remain there, thus stabilizing the lytic state and activation of the lytic P_L and P_R promoters. RexB modulates the effect of RexA and may also help establish phage DNA replication as lytic growth ensues.

Keywords: bacteriophage λ, lysogeny, prophage, lytic growth, phage development, genetic switch

Introduction

λ is a temperate bacteriophage and thus can exist in either the lysogenic or lytic state (H Echols, 1986; Oppenheim, Kobiler, Stavans, Court, & Adhya, 2005). The transition between these two states is mediated by two λ regulators: CI and Cro (Eisen et al., 1975; Ptashne & Hopkins, 1968). In the lysogenic state, the phage chromosome is integrated into that of its host *Escherichia coli* and is quiescent with its lytic functions repressed by the CI protein (Ptashne & Hopkins, 1968). In the repressed lysogen, pairs of CI dimers bind cooperatively to operator sites O_{L1} and O_{L2} on the left and O_{R1} and O_{R2} on the right to repress the early P_L and P_R promoters (Figure 1), respectively, and thereby, inhibit transcription of all the lytic genes downstream from those promoters (A. D. Johnson, Meyer, & Ptashne, 1979). Interaction between CI repressor molecules bound to the left and right operators results in topological looping of the intervening DNA, which contains the phage immunity region (Dodd, Shearwin, & Egan, 2005); this looping enhances repression of P_L and P_R and stabilizes the lysogenic state. In a lysogen, the *c*I repressor gene is transcribed and expressed from the P_{RM} promoter (Spiegelman et al., 1972). When CI repressor is bound to O_{R1} O_{R2}, it activates transcription initiation by RNA polymerase at the P_{RM} promotor (Lewis, Gussin, & Adhya, 2016). Two other genes, *rexA* and *rexB*, are downstream of the *c*I gene and, like *cI*, are expressed as part of the P_{RM} operon (Benzer, 1955; Matz, Schmandt, & Gussin, 1982) (Figure 1). A second promoter, P_{LIT}, is located within the distal end of *rexA*, and transcribes just *rexB* (Hayes, Bull, & Tulloch, 1997; Landsmann, Kroger, & Hobom, 1982). Thus, *rexB* can be transcribed by either P_{RM} and/or P_{LIT} (Hayes & Szybalski, 1973; Liu, Jiang, Gu, & Roberts, 2013; Thomason et al., 2019). A λ lysogen can switch to the lytic pathway, produce progeny phage, and lyse its host, releasing phage. This can happen in response to DNA damage, which in *E. coli* initiates the SOS response (d'Ari, 1985; Witkin, 1991). Single-stranded

DNA is generated as a result of the damage and is bound by the RecA protein, converting RecA to an activated DNA-bound form, RecA*. RecA* binds the CI repressor and acts as a co-protease, initiating auto-cleavage of the CI protein (Craig & Roberts, 1980; Ennis, Ossanna, & Mount, 1989). Loss of CI repression leads to activation of the lytic P_L and P_R promoters. The *cro* gene, which encodes the Cro repressor, is the first transcribed gene from the P_R promoter (H. Echols, Green, Oppenheim, Oppenheim, & Honigman, 1973; Folkmanis, Maltzman, Mellon, Skalka, & Echols, 1977). Cro repressor binds to the same operator sites as CI, but with a different pattern of affinities (Darling, Holt, & Ackers, 2000; A. Johnson, Meyer, & Ptashne, 1978). As Cro repressor is made, it first binds O_{R3} and represses the pRM promoter, thus blocking P_{RM} and *c*I gene transcription, and further reducing CI repressor levels and stabilizing the switch to lytic expression. Thus, Cro locks in the anti-CI repressor state, also called the nonimmune state, ensuring lytic growth (Ptashne et al., 1980; Svenningsen, Costantino, Court, & Adhya, 2005) .

λ cI^+ lysogens, which express wild type CI repressor, are maintained in a repressed state at any growth temperature. A mutation in the *c*I gene, *cI857,* results in a temperature sensitive repressor protein; at lower temperatures at 37°C and below, λ prophages with the *cI857* allele form stable lysogens, and switch to lytic growth at temperatures above 37°C (Sussman & Jacob, 1962). This occurs without any requirement for DNA damage or an SOS response. The *c*I *ind1* allele (Jacob & Campbell, 1959) results in an E117K amino acid change in the CI repressor protein (Gimble & Sauer, 1985) that prevents SOS mediated RecA* coprotease autocleavage of the CI repressor, making the prophage uninducible by DNA damage.

Baek et al. (2003) noticed that a λ lysogen with the *rexA* and *rexB* genes replaced with *gfp* was less inducible at low ultraviolet (UV) doses than a lysogen with *rexA* and *rexB* intact, suggesting that one or both of the Rex proteins have a role in prophage induction. We have further explored the effects of RexA and/or RexB on repression and the induction of λ from the repressed prophage state. Our findings suggest that RexA stabilizes the nonimmune state. RexB appears to antagonize the effect of RexA and may be involved in establishment of the phage DNA replication complex once the transition to lytic growth occurs. Results showing that the Rex system may assist in the establishment of phage replication are found in Supporting Information Results and Discussion and Table S1.

Results

RexA and RexB proteins modulate the level of phage yield in response to UV induction. We compared the ultraviolet inducibility of λ*c*I$^+$ lysogens, defective in RexA and/or RexB functions, to each other and to wild type Rex+ lysogens (Figure 2A). The lysogen defective for RexA function, LT1676, retains the P_{LIT} promoter and expresses RexB fully from both P_{RM} and P_{LIT} (see bacterial strains in Table 1). Relative to a wild type λ *rexA*$^+$ *rexB*$^+$ lysogen (filled circles), the three lysogens defective for Rex function induce less well at low UV doses, but all induce like wild type at the highest doses (Figure 2A). λ *c*I$^+$ lysogens defective for RexA function are very defective for induction at low levels of irradiation irrespective of whether the phage expresses RexB function. In fact, the RexA mutant (open triangles) is as impaired for induction at low UV doses as a lysogen lacking both RexA and RexB functions (open circles). In contrast, the lysogen defective for only RexB function (filled triangles) is similar to wild type in responding to low levels of UV and shows only a modest reduction in levels of phage produced,

i.e., pfu/ml in Figure 2A. In summary, these results demonstrate a positive activity of RexA in promoting induction of the lysogen when switching to the lytic state in response to low levels of DNA damage. There is a small positive effect of RexB when it is co-expressed with RexA. All four lysogens, independent of their *rex* genotype, respond to the same extent to a fully inducing dose of UV (~15 J/m^2) (see Figure 2A). Researchers other than Baek *et al.* (2003) may have missed this effect of Rex functions on UV induction since the historic dose used to induce λ has been ~15 J/m^2 (Coetzee & Pollard, 1974). We also find that expression of RexA and RexB from the arabinose operon can stimulate UV induction of a λ*cI*$^+$ *rexA*$^-$ *rexB*$^-$ lysogen (Figure 2B, open diamonds), confirming that the λ Rex functions can complement *in trans* to alter the basic behavior of the CI /Cro bistable switch when responding to lower levels of UV.

RexA enhances the spontaneous transition to the nonimmune state, as monitored by a P_R *lacZ* reporter. Our data show that the RexA protein stimulates lytic growth and phage production at suboptimal UV doses. We next asked whether the positive effect of RexA on prophage induction requires SOS-induced autocleavage of CI protein by determining whether RexA stimulates when CI repressor is not cleavable, i.e., contains the *ind1* mutation, or in RecA-mutant cells defective for the SOS response. We used the *c*I*857* temperature sensitive repressor allele for these experiments, since Toothman and Herskowitz (1980) previously noticed enhanced Rex-dependent effects in a *c*I*857* repressor background at temperatures where CI-mediated repression is active. Reichardt (Reichardt, 1975) showed that repressor protein levels are higher in *c*I*857* lysogens than in *c*I$^+$ lysogens. This higher level of *c*I*857* protein is made in response to the autoregulatory properties of the P_{RM} promoter in order to maintain a constant

level of CI repression. Thus, more P_{RM} activated transcription will also generate more RexA/B protein and would account for enhanced RexA activity.

E. coli strains containing λ *cI857 ind1* constructs with either the *cro*+ or *cro*$^-$ alleles were modified to carry the four combinations of the *rexA* and *rexB* genes described in the legend of Figure 2A. These eight constructs contain only the phage immunity region as shown in Figure 3 and are nonlethal; such constructs have been described by Svenningsen et al. (2005). Cultures of the Cro$^+$ strains were grown in L broth overnight, diluted and spread for individual colonies on MacConkey Lactose agar. The indicator plates were incubated at low temperature where CI857 repressor is active. After 2-3 days, red papillae formed (Figure 4) in the bacterial colonies, which indicated that within the colony there was a clonal population of cells expressing β-galactosidase from P_R-*c*II-*lacZ* transcripts (see Figure 3). These results suggested that either mutations were occurring within the *c*I repressor gene allowing P_R transcription of *lacZ*, or that an epigenetic change had occurred to lift CI repression and allow Cro repression (Ptashne et al., 1980), i.e., the bistable switch had flipped from the immune state to the lytic state in these papillae. We found that colonies from the two strains having RexA function (LT1886 and LT1891) underwent more papillation than the two strains defective for RexA (LT1887 and LT1892) (Figure 4A), in experiments controlled for temperature and time. Since the non-cleavable *c*I *ind1*$^-$ allele is present in this set of four strains, CI repressor autocleavage is not required for this Rex phenotype. Congruent with this observation, RexA-dependent patterns of papillation occur whether or not the strains are functional for RecA (compare Figure 4A vs 4B). Thus, RexA modulation of the bistable switch does not act through the SOS pathway of CI repressor autocleavage.

158 Confirmation that the rare papillae arise from epigenetic changes rather than from null mutations
159 in the *c*I repressor gene is presented below.
160
161 **A functional Cro gene is required for Rex-dependent papillation.** The Cro repressor is an
162 integral component of the bistable switch and is required for lytic growth (Folkmanis et al.,
163 1977; Lee, Lewis, & Adhya, 2018). We found that the Rex-dependent effects on colony
164 papillation are only observed when Cro function is present. When the $RecA^+$ reporter strains
165 with the four combinations of *rexA* and *rexB* are defective for the Cro repressor, the papillation
166 phenotype becomes independent of Rex function, with papillae occurring at a lower frequency
167 than in the Cro^+ strains (Figure 4C). Sequence analysis of four red papillae from each of the Cro
168 mutant strains revealed the presence of mutations in the *c*I gene which render them unable to
169 maintain the immune state. In contrast, no *c*I mutations were found under $RecA^+$ Cro^+ conditions
170 when four red papillae of each genotype were sequenced.
171
172 **RexA promotes stability of the nonimmune state.** Twenty different papillae from each of the
173 eight strains shown in Figure 4A and 4B were struck on MacConkey Lactose agar for
174 purification. When each of these purified red colonies is grown in L broth and then spread on
175 MacConkey Lactose agar, rare white colonies appear among the red colonies on the plate. Thus,
176 not only do immune (white) colonies contain papillae that have switched to the nonimmune (red)
177 state, but once switched, they can also switch back to the immune (white) state. The percentage
178 of switched white colonies within each culture was determined for each genotype (Figure 5). The
179 most stable nonimmune state is in the cells with wild type RexA and RexB functions present.
180 This is true whether cells are $recA^+$ or $recA^-$, with 0.9% of $recA^+$ (Figure 5A) and 1.7% of $recA^-$

(Figure 5B) cells switching to the immune state. RexA function exerts a strong positive effect to maintain the nonimmune state even in the absence of RexB, with 1.6% of *recA*$^+$ (Figure 5A) and 2.7% of *recA*$^-$ (Figure 5B) cells in each culture reverting to the immune state. Cells lacking RexA function display higher rates of reversion to the immune state whether or not RexB is present and whether or not host RecA protein is present. We observed small differences due to removal of host RecA protein (see explanation in Fig S1 of Supporting Information), but our main observation, that the presence of RexA enhances stability of the lytic state of the bistable switch, is independent of RecA function.

We carried out a similar analysis with Lac$^+$ red papillae arising in the RecA$^+$ *cro27* mutant strains LT1055, LT1395, LT1865, and LT1866, which contain the four combinations of RexA and RexB (see Figure 4C) and are defective for Cro function (Eisen, Brachet, Pereira da Silva, & Jacob, 1970). When the red colonies are grown in L broth and dilutions plated on MacConkey Lactose agar, no white colonies were found among thousands of red colonies. This indicates that the *cro27* Lac$^+$ colonies contain mutations in *c*I, which inactivate repressor function as discussed earlier. Our data indicate that red papillae due to *c*I mutations do occur but compose a small minority of the total papillae under Cro$^+$ conditions, whereas, under Cro$^-$ conditions, we found only *c*I mutations.

RexA$^+$ strains show earlier expression of the P_L lytic promoter during the transition to the nonimmune state. We looked for Rex-dependent transcription differences in expression of a reporter gene under control of the lytic promoter P_L during transition of the bistable switch to the lytic state. Strains LT1657, LT1659, LT1895 and LT1897 are similar to those used for the

papillation experiment (Figure 4A) but contain a wildtype CI repressor ($cI^{+}ind^{+}$); thus, in these strains, the nonimmune state is inducible by DNA damage but not by high temperature.

A low dose of Mitomycin C (MC) was added to log phase cultures of these strains to cause DNA damage and trigger RecA*-dependent autocleavage of CI repressor and activation of P_L- and P_R-mediated transcription. Once induced by MC, Cro expression from P_R results in repression of P_{RM}, completing the switch from the lysogenic to the lytic state. The results are shown in Figure 6.

The effect of RexA and/or RexB function on expression of luciferase from the lytic promoter P_L was monitored over time in the four different strains. The CI and Cro repressors were wild type in all cases. When RexA function is present and RexB is absent (Figure 6A, strain LT1895, open triangles), luciferase expression from the lytic promoter P_L occurs reproducibly earlier than when both RexA and RexB are absent (strain LT1897, open circles); this again demonstrates the positive effect of RexA on the transition to the lytic state. In contrast, when RexB function is present and RexA is absent (Figure 6B, strain LT1659, closed triangles), the kinetics of luciferase expression from P_L are similar to those observed when both RexA and RexB are absent. Thus, expression of RexB alone does not alter the timing of P_L activation. However, when both RexA and RexB proteins are present (Figure 6C, strain LT1657, closed circles), P_L expression is delayed relative to the strain with only RexA function (open triangles). Thus, when present, RexB can inhibit RexA stimulation of luciferase from P_L. This experiment illustrates the independent and opposing effects that RexA and RexB have on the transition to the lytic state by affecting the timing of expression of the lytic P_L promoter. Note that the earliest time points

show no genotypic differences, suggesting that RexA does not act until DNA damage has occurred, CI repressor levels are reduced, and prophage induction has begun.

Rex effects on spontaneous phage release of *c*I*857 ind1* lysogens: We have shown that RexA function stimulates switching from the immune to the nonimmune state when Cro function is present by monitoring the expression of reporter genes from the major rightward (P_R) and leftward (P_L) lytic promoters in a defective prophage. We next looked for effects of Rex function on the bistable immunity switch in λ lysogens carrying a complete prophage. λ lysogens, when grown in culture, are relatively stable and rarely release phage. There is, however, a low level of phage release. Some of the phage released are rare *c*I mutants that have simply lost repressor activity, but the vast majority are genetically identical to the original prophage and arise from a cell in which λ had switched from the immune to the non-immune state; the two types are distinguishable by plaque morphology (Little & Michalowski, 2010). We tested the effects of RexA and/or RexB on this spontaneous phage release using *c*I*857* lysogens with the *ind1* mutation to block SOS-mediated prophage induction (see Figure 7).

We find that RexA enhances the transition to lytic growth. This RexA effect is most evident in the absence of RexB function (Figure 7, compare LT2320 and LT2321), where removal of RexA activity by mutation results in a >7-fold reduction in free phage titer. As observed previously, this RexA effect is nearly absent when RexB function is present: compare the *rexA*$^+$ LT1684 with the *rexA* mutant LT2319; the levels of free phage in these two lysogens varies by <2-fold (see Figure 7). Clear plaques result from *c*I mutations that prevent lysogeny and account for less than 5% of the total phage yield for all genotypes. Thus, while demonstrating the positive effect

of RexA protein on the transition to lytic growth, the data also reveal that RexB protein antagonizes RexA function.

Two-hybrid analysis of protein-protein interactions between RexA, RexB and the CI and Cro repressors. Protein-protein interactions occurring between RexA, RexB, and the phage repressors CI and Cro might affect the operation of the bistable switch. Thus, we looked for such interactions using the Bacterial Adenylate Cyclase Two Hybrid (BACTH) system (Karimova, Gauliard, Davi, Ouellette, & Ladant, 2017; Ouellette, Karimova, Davi, & Ladant, 2017). This two-hybrid analysis is performed in an *E. coli cya* mutant lacking adenylate cyclase function, using compatible plasmids expressing the T25 and T18 adenylate cyclase domains from *Bordatella pertussis* fused to either the N- or C-terminus of proteins of interest. Interaction between the two proteins being tested results in association of the two cyclase domains, giving cyclase activity and consequent cAMP production. We previously used this system to show that RexA and RexB interact with themselves and each other (Thomason et al., 2019). For that study we generated eight plasmids that express the *rexA* and *rexB* genes fused in frame at either the N- or C-terminus to each of two different cyclase domains. Here we made eight additional plasmids by inserting the phage repressor genes, *c*I and *cro*, into the four cyclase vectors in the same manner. We then introduced plasmid pairs to be tested for interaction into the *cya* mutant host, BTH101 (Table S2 A-E). To ensure that only meaningful interactions were included in the analysis, we first screened strains with the pairs of plasmids for the ability to confer growth on minimal maltose (see pictures accompanying Table S2 A-E), since activation of the *mal* genes depends strongly on cAMP (Raibaud, Vidal-Ingigliardi, & Kolb, 1991). We then measured β-galactosidase production from the bacterial *lacZ* gene for each of these positive plasmid pairs,

since expression of the *lac* operon also requires cAMP for promoter activity (see Table 2). The results confirm that both RexA and RexB proteins interact with the CI repressor. For RexA and CI, only proteins with N-terminal cyclase tags allowed growth on maltose, suggesting that the C-terminal domains of these two proteins interact. It is known that CI repressor dimers form via an interaction domain located in the repressor C-terminus (Beckett, Burz, Ackers, & Sauer, 1993; Burz & Ackers, 1994). Thus, it is not surprising that these CI hybrid proteins form dimers with the cyclase tag on the N-terminus. Robust β-galactosidase values suggest that CI repressor with an N-terminal cyclase tag also interacts well with RexB protein. The cyclase tags can be at either end of RexB, which is an inner membrane protein, and predicted to have both N- and C- termini in the cytoplasm (Parma et al., 1992). β-galactosidase assays testing interaction of the Cro repressor with RexA and RexB proteins (Table 2) show about half the level of signal that we found for CI repressor-RexA/B interaction.

The plasmids expressing the hybrid CI repressor confer immunity to λ, demonstrating that the CI fusion proteins are able to bind to the operator sites at the lytic promoters. Since binding to the operators might change protein-protein interactions and thus the β-galactosidase results, we tested a subset of the plasmid pairs in a derivative of the *cya* mutant strain having the phage operator sites present on the bacterial chromosome. However, we saw no significant differences in β-galactosidase levels with or without the repressor operator sites present (see Table 2, LT2333 vs LT2446 and LT2331 vs LT2447).

RexA is a non-specific DNA binding protein that forms stable complexes with CI oligomers *in vitro*. Our BACTH data demonstrate that RexA and RexB can associate with CI *in vivo*. To

study these interactions directly, we sought to purify RexA and RexB recombinantly from *E. coli* and test whether they could bind CI *in vitro*. RexA can be purified in milligram quantities as a soluble, monodispersed dimer (Figure 8A). We observe no evidence of subunit exchange in solution, suggesting that dimerization occurs during protein folding and the dimer remains stably associated. All attempts to purify RexB were unsuccessful, regardless of the tag used or how the protein was expressed.

Analytical size exclusion chromatography (SEC) shows that purified CI repressor elutes earlier than the RexA dimer under the same experimental conditions (Figure 8B, gels I and II), consistent with the ability of CI to form larger oligomers (Bell, Frescura, Hochschild, & Lewis, 2000; Dodd, Perkins, Tsemitsidis, & Egan, 2001; Révet, von Wilcken-Bergmann, Bessert, Barker, & Müller-Hill, 1999; Stayrook, Jaru-Ampornpan, Ni, Hochschild, & Lewis, 2008). When the assembled CI multimers are mixed with RexA dimers, a portion of RexA co-elutes with CI and both proteins are enriched in the heaviest, early fractions (8B, gel III versus I and II), indicating that RexA can form stable complexes with CI in solution.

CI also forms complexes with double-stranded DNA (dsDNA) containing either the λ O_L or O_R operator sequences (Figure 8B, gels I, IV, and V and gels I, VIII, and IX), as evidenced by the leftward shift of the DNA bands when CI is added (Maniatis & Ptashne, 1973). Surprisingly, RexA also shifts to a larger species in the presence of these substrates (Figure 8B, gels II, IV, and VI and gels II, VIII, and X; Supporting Information Figure S1B, gels I, II, and III), implying that RexA also binds dsDNA. Further examination by filter binding shows that RexA preferentially associates with dsDNA compared to single-strand DNA (ssDNA) (Figure 8C, O_R1-

O_R2 vs. ssO_R1-O_R2) but lacks sequence specificity for the λ operator region (O_R1-O_R2 vs. O_R1-O_R2 scrambled). RexA and CI form ternary complexes on both O_L and O_R operator DNA substrates with no significant changes to the overall elution profile of the individual components (Figure 8B), signifying that the abilities of RexA to bind CI and DNA are not mutually exclusive.

We next assessed whether CI oligomerization is a prerequisite for RexA binding. Previous biochemical and crystallographic studies showed that the CI missense mutation D197G (Supporting Information Figure S2A) yields stable CI dimers that retain the ability to bind single operator sites but are impaired in higher order assembly and cooperative repressor functions (Stayrook et al., 2008; Whipple, Kuldell, Cheatham, & Hochschild, 1994). Purified CI D197G dimers form stable complexes with O_L1-O_L2 operator DNA substrates (Supporting Information Figure S2B, gels I, IV, and V). However, we observe no significant shift in either protein when CI D197G is incubated with RexA (Figure S2B, gels II, IV, and VI). When operator DNA substrates are added to this mixture, the elution fractions overlay with positions of the individual RexA-DNA and CI D197G-DNA complexes (Figure S2B, gels I, III, V, and VII), arguing against the formation of a ternary complex. No stable complexes are formed between RexA and either the purified CI NTD or CTD domains, respectively (Figure S2C). Together these data argue that RexA is a non-specific DNA binding protein that can specifically bind assembled CI oligomers.

Discussion

The two basic components of the phage λ bistable switch are the CI and Cro repressor proteins that bind to operator sites flanking the major lytic promoters, P_L and P_R, to regulate gene expression. RexA and RexB proteins are certainly not required for the λ bistable switch; however, our results suggest that they are accessory factors able to modulate switch activity, providing an additional layer of regulation that refines the ability of the virus to maintain lysogeny or exit from the lysogenic state. RexA potentiates induction when the inducing signal is low by stabilizing the transition to the lytic state. Some of our experiments show an antagonistic effect of RexB on this RexA-mediated activity (Figures 6,7). Induction is optimal when both RexA and RexB are present (Figure 2), while lysogens mutant for both RexA and RexB are the least prone to transition to the non-immune state (Figures 2, 4, 7). In this way, RexA and RexB act together as two opposing forces to modulate the switch between lysogenic and lytic growth, reducing stochasticity in the switch (Arkin, Ross, & McAdams, 1998; Bednarz, Halliday, Herman, & Golding, 2014; Golding, 2011). Once the bistable switch has transitioned to the non-immune state, our data show that only RexA is necessary to stabilize the lytic configuration and reduce the tendency to return to the immune state (Figure 5). Since RexA is not expressed when the switch is in the nonimmune state, we presume that some P_{RM} expression must be required before RexA can act in the experiments shown in Figure 5 (see Figure 9).

Two types of models may explain Rex effects: Rex proteins either act to directly affect λ behavior, or the Rex proteins alter cell physiology, and this altered physiology in turn affects λ behavior. Our data support the first model, since we demonstrate a direct interaction between the Rex proteins and the phage repressors (Table 2), as well as between the Rex proteins and the phage replication proteins O and Ren (Table S1). Although the Rex system can have energetic

effects on the cell, those effects require both Rex proteins (Matz et al., 1982; Parma et al., 1992; Snyder & McWilliams, 1989). Data presented here clearly show that RexA alone exerts an effect on the bistable switch.

Our genetic and biochemical analyses demonstrate that RexA physically interacts with the CI repressor both *in vivo* and *in vitro*. *In vivo*, this interaction was confirmed in the bacterial two-hybrid system as measured by the ability to activate cAMP-dependent promoters. These results suggest that the two proteins can interact via their C-terminal domains. *In vitro*, purified RexA dimers form stable complexes with assembled CI multimers and also bind both dsDNA and ssDNA non-specifically. RexA and CI form ternary complexes on DNA substrates containing λ operator sites, arguing that RexA does not directly inhibit CI intrinsic DNA binding capability, nor does it compete for the same binding sites, which would restrict repressor access. We see no evidence of RexA-mediated CI cleavage analogous to that mediated by RecA protein. We hypothesize that *in vivo*, RexA, facilitated by its interactions with DNA and CI, is present at the λ P_L and P_R promotors regulated by CI repressor, where it reduces the ability of CI to establish tight repression, thus pushing the system toward the lytic state (see Figure 10).

RexB is an integral inner membrane protein with four predicted transmembrane segments and three charged cytoplasmic loops; thus, these loops are poised to associate with different binding partners in the cytoplasm (Figure 11) (Krogh, Larsson, von Heijne, & Sonnhammer, 2001; Parma et al., 1992). We find an interaction between RexB and CI repressor in the two-hybrid study (Table 2), suggesting that in a repressed lysogen, CI repressor, bound at its operator sites, may be localized at the inner surface of the cytoplasmic membrane via non-covalent interactions

with RexB. CI requires an N-terminal cyclase tag to interact with RexB, however, the cyclase tag on RexB can be at either the N- or C-terminus. Thus, the CI-RexB interaction likely occurs via the RexB central cytoplasmic loop (Figure 11). We previously showed that RexA and RexB physically interact *in vivo* (Thomason et al., 2019); the strength of the RexA-RexB interaction is similar to that of RexA with CI (Table 2). The antagonistic effect of RexB on RexA activity may occur because RexB association with CI bound to the operator sites at the inner membrane makes CI less available to RexA, deepening repression. Alternatively, RexB may titrate RexA, reducing the amount of free RexA protein available to interact with CI and DNA. Regardless of how RexB acts at the molecular level, RexA and RexB must function together to optimize modulation of the CI/Cro bistable switch, with each protein having independent and complementary effects as the phage switches from lysogenic development to lytic growth (see Figure 10).

RexB continues to be transcribed from P_{LIT} after prophage induction as the lytic promoters P_L and P_R become active (Fig. 1). The genes encoding the phage DNA replication functions, O and P, are transcribed from P_R. Our two-hybrid analysis (Table S1) suggests a strong physical interaction between the RexB and λ O proteins, consistent with the observation that intracellular RexB stabilizes O protein *in vivo* (MacHattie, 1985; Schoulaker-Schwarz, Dekel-Gorodetsky, & Engelberg-Kulka, 1991). Interaction between RexB and O could tether the phage replication complex to the inner membrane, with RexB serving as a central hub to localize phage DNA replication as well as to coordinate the transition from lysogeny to lytic growth (see Supplementary Results and Discussion).

This work has defined novel and complementary roles for the phage λ RexA and RexB proteins in the switch from lysogeny to lytic growth. Previously, the Rex system was thought to function solely in the lysogenic state to exclude infecting phages such as T4*r*II by triggering cellular energetic defects (Benzer, 1955; Gussin & Peterson, 1972; Matz et al., 1982; Parma et al., 1992). Given its location at the inner membrane, we suspect that the Rex system may sense and respond to the energetic state of the cell, and exclusion may occur as a byproduct.

Despite serving as the basis for pioneering studies in molecular biology and genetics (Benzer, 1955; Crick, Barnett, Brenner, & Watts-Tobin, 1961), the Rex system has long been considered a unique outlier among bacteriophage. The explosion of genome sequencing in recent years, however, has unearthed putative *rex*-like genes in numerous temperate *Mycobacterium* and *Gordonia* phages (Russell & Hatfull, 2017). Homologs from phages Sbash, CarolAnn, and Butters confer a broad viral defense that mirrors the Rex exclusion behavior in λ (Gentile et al., 2019; Mageeney et al., 2020; Montgomery, Guerrero Bustamante, Dedrick, Jacobs-Sera, & Hatfull, 2019). These genes are organized in tandem in a single operon that is often directly adjacent to a CI-like repressor gene, raising the tantalizing possibility that other bacterial viruses also use these analogous systems to fine tune the balance between lysogeny and lytic growth. Future studies will determine the generality of this mechanism and continue the legacy of bacteriophage λ (Golding, 2016) and the Rex system as important experimental platforms.

Experimental Procedures

Materials and Media: Bacterial cultures were grown in L broth containing 10g tryptone, 5g yeast extract and 5g NaCl per liter, and on L plates, which contained ingredients above and 1.5%

433 Difco agar. Cultures for plating phage were grown to exponential phase in tryptone broth
434 containing 10g tryptone, 5g NaCl, and 10mM $MgSO_4$ per liter. Phage stocks were maintained in
435 TMG, containing 10mM Tris base, 10 mM $MgSO_4$ and 0.01% gelatin, pH7.4. Phage were
436 enumerated on tryptone plates 10g tryptone and 5g NaCl per liter using 0.25 ml of fresh plating
437 cultures mixed with 2.5 ml melted tryptone top agar (0.7% agar) containing 10 g tryptone and 5
438 g NaCl. MacConkey Lactose agar medium was from Difco and contained 1% lactose and 1.35%
439 agar. Dilutions of bacteria were made in M9 Salts, dilutions of phage were made in TMG.
440
441 Bacterial strains used for most experiments are in Table 1, those used for the BACTH analysis
442 are in Table 2. Strains were constructed using a combination of recombineering and P1
443 transduction methods (Thomason, Costantino, & Court, 2007; Thomason, Sawitzke, Li,
444 Costantino, & Court, 2014). Sequences of single-strand oligonucleotides used for
445 recombineering are available upon request. The mutations to inactivate *rexA* and *rexB*
446 individually or together are described in Thomason et al. (2019). Briefly, most of each gene was
447 removed and replaced with the open reading frame of a selectable drug marker, but two regions
448 were left intact: the distal end of the *rexA* gene, which contains the P_{LIT} promoter; and the distal
449 end of the *rexB* gene, which is necessary for optimal transcriptional termination at the intrinsic
450 terminator for the immunity region, T_{IMM}, which is immediately downstream of *rexB*. For
451 simplicity these mutations are simply indicated in the strain list (Table 1) as *rexA* and *rexB* drug
452 marker replacements. Once the *rex* mutations were inserted in the intact prophage, lysogenic
453 candidates were screened by cross-streaking against a *c*I mutant phage, and those that displayed
454 immunity were further screened with a PCR test (Powell, Rivas, Court, Nakamura, &
455 Turnbough, 1994) to identify monolysogens, which were used for all analyses.

456

457 *UV induction of λ lysogens:* Overnight cultures of lysogens and strain A584 for titering released
458 phage were grown in LB at 32 C overnight. Lysogens were diluted 1/500 into 35 ml LB and
459 grown in a 32ºC shaking water bath to an OD_{600} of approximately 0.15. Then 30 ml of the cells
460 was harvested by centrifugation and suspended gently in 1 ml of TMG. 29 ml TMG was added,
461 and the wash and suspension steps repeated. After the second wash, 14 ml TMG was added to
462 the cells, for a total of 15 ml, resulting in a two-fold concentration and ~$2x10^8$ cells/ml in TMG.
463 The washed lysogenic cells were placed in a sterile empty petri dish and working under a red
464 light, were irradiated with UV for the indicated amount of time. Every 5 seconds, 100 µl was
465 withdrawn and dispensed into a sterile Eppendorf tube, out to 30 sec. 10 microliters from each
466 Eppendorf was added to 10ml LB in a 50ml baffled flask. Cells were incubated in the dark in a
467 37ºC shaking water bath for two hours. Serial dilutions of the resulting lysates were made and 10
468 µl of each dilution was spotted on a lawn of A584 poured onto TB plates; the dilutions were
469 stored overnight. The next day the approximate titers of each dilution were estimated from the
470 spot plates, and more accurate titers determined as follows: 50 or 100µl of the appropriate phage
471 dilution was mixed with 0.25 ml A584 in a small plating tube, this cell-phage mix remained at
472 room temperature for at least 10 min, then 2.5 ml melted TB top agar was added, and the
473 contents immediately poured on a TB plate. Once the top agar hardened plates were inverted and
474 incubate overnight at 37ºC. The next day, the number of plaques on each plate was counted and
475 titers were determined for each UV time point. Plating bacteria were made by diluting the A584
476 overnight 33-fold into five ml tryptone broth containing 10mM MgSO4, growing for 2.5 hrs at
477 32ºC with aeration, after which five ml of TMG (10mM Tris 10mM MgSO4 10mM gelatin) was
478 added. This thin culture was used to assay released phage.

Papillation assays: The papillation of strains carrying the dual $P_L P_R$ reporters with a *cI857 ind1* allele and *rexA* and *rexB* mutations was examined by plating appropriate dilutions of fresh LB overnight cultures on MacConkey-Lactose to obtain isolated single colonies. MacConkey-Lactose petri plates were incubated at 32-34°C until papillae arose within individual colonies (Fig. 4). All plates in a set were incubated under identical conditions. Once papillae developed, the plates were photographed, and the pointed end of a small pipette tip was used to pick individual papillae and purify them to single red colonies on MacConkey-Lactose; these plates were incubated at 30°C degrees. Twenty-four independent red colony isolates of each genotype were propagated in this fashion for the $RecA^+$ strains, and eighteen for the $RecA^-$. Once these red colonies were purified away from white colonies, overnight cultures from the red colonies were grown in L broth at 30°C and plated on MacConkey-Lactose solid agar for single colonies. After overnight incubation at 30°C, colonies were counted for each independent culture and the number of red and white colonies tabulated. The percentage of white colonies among reds was determined for each genotype (Fig. 5). In every case, a few colonies of each genotype failed to give any white colonies. Such non-reverting red colonies likely contain mutations in the *c*I repressor gene, which generate inactive CI repressor protein; these were not included in the analysis. The final number of colonies analyzed is indicated in the legend to Fig. 5. Numerical data are shown in Supporting Information Table S4; these data were used to generate the bar graphs shown in Fig. 5A and 5B.

Kinetics of induction monitoring P_L N-luc reporter. Overnight cultures of strains LT1657, LT1659, LT1895, and LT1897 were grown in L broth from single colonies. Cultures were

diluted 500-fold into 25ml L broth in 125 ml baffled flasks in a 37ºC shaking water-bath. After 1.5 hrs, 1.0 ml samples were withdrawn from the flasks and 3ng/ml Mitomycin C (MC) was added to each flask. For these and subsequent samples, taken every 30 min, the A600 was determined, and luciferase assays were performed immediately, using the Promega Luciferase Assay System (catalog no. E1500) according to the company's directions. Culture aliquots in L broth (0.1ml) were added directly to 0.4 ml of Cell Culture Lysis Reagent with 2.5mg/ml BSA and 1.25 mg/ml lysozyme. Cell lysate (25µl) was mixed with 0.1ml of luciferase substrate (Promega Luciferase Assay Reagent, catalog no. E151A), incubated for 2.0 min and read in a BD Pharmingen Monolight 3010 single sample luminometer for 10s. Each sample was assayed in duplicate. The relative light unit (RLU) was normalized to the A600. Three biological replicates of the experiment were performed, one representative experiment is shown (Figure 6).

Analysis of spontaneous phage release in lysogenic cultures: Lysogenic cells were first washed to remove viral particles: five ml overnight cultures of lysogenic strains were pelleted in the Sorvall at 6700rpm for 7min. Pellets were suspended in 1ml TMG, additional TMG was added to ~25ml total volume, and suspensions were mixed by vortexing. Cells were again pelleted, suspended in TMG, and pelleted as before, then the cell pellet was suspended at the original 5ml volume and diluted 1/400 into 10ml L broth in 125ml baffled flasks. Aliquots (1ml) of each genotype were removed and filtered with a 0.2µm filter; 0.3ml of the filtered lysate was plated on tryptone plates using C600 as host to determine initial phage titer, which was negligible in all cases. Cultures were incubated with shaking in a 32°C water bath until the OD_{600} was 0.2-0.3. Final OD_{600} was determined for each culture and the number of viable cells per ml was determined from colony counts obtained by plating dilutions of lysogenic cultures on L agar petri

plates and incubating plates overnight at 32°C. 1.5ml each culture was removed and filtered with a 0.2µm filter, three 10-fold serial dilutions into TMG were made for each of the filtered lysates. 0.25ml of C600 plating culture was mixed with 2.5ml melted tryptone top agar and poured onto tryptone petri plates. Once plates hardened, 10µl of the undiluted lysate and each dilution was spotted on the surface of the lawn. Plaques in each 10µl spot were counted to determine approximate titers of the cultures. These approximations were used to guide the selection of appropriate dilutions of filtered lysates to determine an accurate number of phage particles in the supernatants. Both clear (c^-) and turbid (c^+) plaques were enumerated. Clear plaques result from mutations in the phage that prevent lysogeny and accounted for less than 5% of the total phage yield for all genotypes. Numerical data are shown in Supporting Information Table S5.

Two-hybrid analysis: The Bacterial Adenylate Cyclase Two Hybrid System Kit (BACTH Kit) from Euromedex (www.euromedex.com) was used to look for protein-protein interactions between the RexA and RexB proteins and the two phage repressor proteins in *E. coli*. Construction of *rexA* and *rexB* plasmids was previously described (Thomason 2019). Recombineering was used to insert the *c*I and *cro* repressor genes into the four two-hybrid vectors: the low-copy KanR pKT25 and pKNT25 plasmids with the T25 adenylate cyclase domain on the N- and C-terminal domains fused in frame to the gene of interest, respectively. The two repressor genes were also inserted into the high-copy AmpR pUT18 and pUT18C plasmids, with the T18 adenylate cyclase domain fused in frame to the C- and N-terminal domains of the gene of interest, respectively. For BACTH complementation assays, various pairs of T25 (KanR) and T18 (AmpR) plasmids were introduced into the *cya* mutant strain BTH101 by co-electroporation. The BTH101 derivatives containing these plasmid pairs are listed in Table

548 S2 A-E of the Supporting Information. After outgrowth, 10µl drops of ten-fold serial dilutions of
549 the transformed cells were spotted onto petri plates containing L agar with kanamycin (30µg/ml),
550 ampicillin (100µg/ml) and X-gal (50µg/ml). Plates were incubated at 32°C overnight. Colonies
551 from these petri plates were subsequently purified on M63 minimal maltose solid agar containing
552 the same drugs plus 1mM IPTG. Growth on minimal maltose indicated cAMP-dependent sugar
553 utilization and thus a positive interaction between the two phage proteins being tested; such
554 interaction results in interaction of the two fused adenylate cyclase domains (Supporting
555 Information Table S1). Out of 51 strains tested, 13 grew on minimal maltose, and β-
556 galactosidase assays were used to provide an estimate of the strength of interaction for these
557 pairs of plasmid-borne phage proteins (Table 2). For these assays, colonies picked from the
558 minimal maltose agar plates were used to generate overnight cultures grown in L broth
559 containing the same antibiotics at the same concentrations. The day of the assay, cells were
560 diluted 100-fold into L broth lacking antibiotics and β-galactosidase assays were done according
561 to Thomason et al. (2019). At least three independent cultures were measured for each plasmid
562 pair. A similar protocol was followed for the phage O, P, and Ren proteins (see Supporting
563 Information Results and Discussion and Table S1).
564
565 *Cloning, expression, and purification of bacteriophage λ RexA and CI constructs:* DNA
566 encoding the full-length bacteriophage λ RexA (UniProt P68924) and CI (UniProt P03034)
567 proteins were codon optimized for *E. coli* expression and synthesized commercially by Bio Basic
568 Inc. The DNA encoding full-length RexA (residues 1-279) was amplified by PCR and cloned
569 into pET21b, introducing a 6xHis tag at the C-terminus. DNA encoding full-length CI (residues
570 1-237), as well as its N-terminal DNA binding domain (NTD, residues 1-93) and the C-terminal

multimerization domain (CTD, residues 133-237), was separately amplified by PCR and cloned into pET21b. The D197G mutation was introduced into full-length CI via the Quikchange Mutagenesis Kit (Agilent). All RexA and CI constructs were transformed into BL21(DE3) cells, grown at 37°C in Terrific Broth to an OD600 of 0.7-0.9, and then induced with 0.3 mM IPTG overnight at 19°C. Cells were pelleted, washed with nickel loading buffer (20 mM HEPES pH 7.5, 500 mM NaCl, 30 mM imidazole, 5% glycerol (v:v), and 5 mM β-mercaptoethanol), and pelleted a second time. Pellets were typically frozen in liquid nitrogen and stored at -80°C for later use.

Thawed 500 ml pellets of each RexA and CI construct were resuspended in 30 ml of nickel loading buffer supplemented with 5 mg DNase, 5 mM $MgCl_2$, 10 mM PMSF, and a Roche complete protease inhibitor cocktail tablet. Lysozyme was then added to a concentration of 1 mg/ml and the mixture was incubated for 10 minutes rocking at 4°C. Cells were disrupted by sonication and the lysate was cleared via centrifugation at 13 000 rpm (19 685 g) for 30 minutes at 4°C. The supernatants were each filtered through a 0.45 μm filter, loaded onto a 5 ml HiTrap chelating column charged with $NiSO_4$, washed with nickel loading buffer, and then eluted via an imidazole gradient from 30 mM to 1 M. Pooled RexA fractions were further dialyzed overnight at 4°C into S loading buffer (20 mM HEPES pH 7.5, 50 mM NaCl, 1 mM EDTA, 5% glycerol (v:v), and 1 mM DTT) and then loaded onto a 5 ml HiTrap SP column equilibrated with S loading buffer. The SP column was washed in the same buffer and then RexA was eluted with a NaCl gradient from 50 mM to 1 M. Peak fractions from the SP column were pooled, concentrated, and further purified by size exclusion chromatography (SEC) using a Superdex 75

16/600 pg column. RexA protein was exchanged into a final buffer of 20mM HEPES pH 7.5, 150mM KCl, 5 mM $MgCl_2$, and 1mM DTT during SEC and concentrated to 10-70 mg/ml.

The chelating column elution fractions containing CI protein were pooled, concentrated, and further purified directly by SEC using either a Superdex 200 16/600 pg column (full-length wildtype) or Superdex 75 16/600 pg column (D197G mutant, NTD, and CTD). CI proteins were exchanged into a final buffer of 20mM HEPES pH 7.5, 150mM KCl, 5 mM $MgCl_2$, and 1mM DTT during SEC and concentrated to 10-40 mg/ml.

Size exclusion chromatography coupled to multi-angle light scattering (SEC-MALS): Purified RexA at 4 mg/mL was subjected to size-exclusion chromatography (SEC) using a Superdex 75 10/300 column (GE) equilibrated in SEC buffer (20 mM HEPES pH 7.5, 150 mM KCl, 5 mM $MgCl_2$, and 1mM DTT). The column was coupled to a static 18-angle light scattering detector (DAWN HELEOS-II) and a refractive index detector (Optilab T-rEX) (Wyatt Technology). Data were collected continuously at a flow rate of 0.5 mL/min. Data analysis was carried out using the program Astra VI. Monomeric BSA at 4 mg/mL (Sigma) was used for normalization of the light scattering detectors and data quality control.

Preparation of DNA substrates from oligonucleotides: All DNA oligonucleotides were synthesized commercially by Integrated DNA Technologies (IDT). Lyophilized single-stranded oligonucleotides were resuspended to 1 mM in 10 mM Tris-HCl and 1 mM EDTA and stored at minus 20°C until needed. For filter binding, single-stranded oligonucleotides were 5’ end-labeled with [γ32P]ATP using polynucleotide kinase (New England Biolabs) and then purified on a P-30

spin column (BioRad) to remove unincorporated label. Duplex DNA substrates were prepared by heating equimolar concentrations of complementary strands (denoted as 'us' and 'ls' indicating upper and lower strands) to 95°C for 15 minutes followed by cooling to room temperature overnight and then purification on an S-300 spin column (GE) to remove single stranded DNA. Sequences for all substrates can be found in Supporting Information Table S3.

Analytical size exclusion chromatography (SEC): 50 µl samples containing full-length CI protein at 125 µM, RexA protein at 125 µM, or a 1:1 mixture of both proteins was incubated for 15 minutes at room temperature and analyzed by SEC using a Superdex 200 PC 3.2 column (GE Healthcare) equilibrated in SEC buffer (20 mM HEPES, pH7.5, 150 mM KCl, 5 mM $MgCl_2$, and 1mM DTT). To assess CI and RexA interactions with DNA, samples containing the annealed double-stranded DNA substrates OR_1-OR_2 or OL_1-OL_2 were also prepared at 2:1.2 protein to DNA molar ratio. Individual DNA substrates were injected alone at a concentration of 75 µM for comparison. All eluted fractions were further analyzed by SDS-PAGE using 4 –20% gradient gels, and then silver-stained to visualize DNA and Coomassie-stained to visualize protein. Samples were similarly prepared for the D197G, NTD, and CTD CI constructs but were analyzed using a Superdex 75 PC 3.2 column (GE Healthcare) equilibrated in SEC buffer.

Filter binding: Filter binding assays were carried out in buffer containing 25 mM MES (pH 6.5), 2.0 mM MgCl2, 0.1 mM DTT, 0.01 mM EDTA, and 40 µg/mL BSA. Binding was performed with wildtype RexA at 30°C for 10 min in a 30 µL reaction mixture containing 14.5 nM unlabeled DNA and 0.5 nM labelled DNA. Samples were filtered through KOH-treated nitrocellulose filters (Whatman Protran BA 85, 0.45 µm) using a Hoefer FH225V filtration

639 device for approximately 1 min. Filters were subsequently analyzed by scintillation counting on
640 a 2910TR digital, liquid scintillation counter (PerkinElmer). All measured values represent the
641 average of at least three independent experiments (mean ± standard deviation) and were
642 compared to a negative control to determine fraction bound.
643
644 **Acknowledgements:** We thank Brenda Shafer for expert technical assistance, Alison Rattray for
645 statistical analyses, and Nina Costantino for critical reading of the manuscript. L.C.T. thanks
646 Nathan Brown for insightful discussions about the Rex system. We also thank Richard
647 Fredrickson and Jonathan Summers at NCI-Frederick Scientific Publications, Graphics, and
648 Media for expert assistance with photography, and M. Spencer, N. Shrader, T. Hartley, and K.
649 Pike from the CRTP Genomics Laboratory of the Frederick National Lab for Sanger sequencing.
650 This work was supported, in part, by the Intramural Research Program of the National Institutes
651 of Health, National Cancer Institute, Center for Cancer Research. This project has been funded
652 in whole or in part with federal funds from the National Cancer Institute, National Institutes of
653 Health, under contract HHSN26120080001E. The content of this publication does not
654 necessarily reflect the views or policies of the Department of Health and Human Services, nor
655 does mention of trade names, commercial products, or organizations imply endorsement by the
656 U.S. Government. This research was supported [in part] by the Intramural Research Program of
657 the NIH, National Cancer Institute, Center for Cancer Research. M.C.A. is supported by a NIFA
658 predoctoral fellowship (2020-67034-31750).
659
660 **Author Contributions:** L.C.T. performed genetic experiments and wrote the manuscript, C.C.
661 performed genetic experiments. C.J.S., C.J.H., and M.C.A. performed biochemistry experiments,

J.S.C. designed biochemical experiments, provided guidance and financial support, and edited the manuscript. D.L.C. provided financial support and guidance and edited the manuscript.

Data Availability Statement.

The data that support the findings of this study are available from the corresponding author upon reasonable request.

668 **Table 1. *Escherichia coli* K-12 Strains**

Strain	Relevant Genotype	Reference/construction
A584	YMC [*trp::*Tn*10 tyrT* (*supF*)]	D. Ennis via F. W. Stahl
C600	*tonA21 thi-1 thr-1 leuB6 lacY1 rfbC1 fhuA1 glnV44 (supE)*	D. Court laboratory
LT445	MG1655(λ *cI*$^+$ *rexB*$^+$*rexA*$^+$) monolysogen	Thomason et al., 2019
LT1055	MG1655 *ΔlacI-kan luc-N pLoL rexB*$^+$ *rexA*$^+$ *cI857ind1 pRoR cro27 cII-lacZYA*	this work
LT1395	MG1655 *ΔlacI-kan luc-N pLoL rexB*$^+$ *rexA<>cat cI857ind1 pRoR cro27 cII-lacZYA*	this work
LT1657	MG1655 *ΔlacI-kan luc-N pLoL rexB*$^+$ *rexA*$^+$ *cI*$^+$ *pRoR cro*$^+$ *cII-lacZYA*	
LT1659	MG1655 *ΔlacI-kan luc-N pLoL rexB*$^+$ *rexA<>cat cI*$^+$ *pRoR cro*$^+$ *cII-lacZYA*	
LT1676	MG1655(λ*cI*$^+$*ind*$^+$ *rexB*$^+$*rexA<>cat*) monolysogen	Thomason et al., 2019
LT1677	MG1655(λ*cI*$^+$*ind*$^+$*rexB<>cat rexA*$^+$) monolysogen	Thomason et al., 2019
LT1678	MG1655(λ*cI*$^+$*ind*$^+$ *(rexAB)<>cat*) monolysogen	Thomason et al., 2019

LT1684	MG1655(λ *cI857 ind1 rexB*$^+$*rexA*$^+$) *lamB<>kan* monolysogen	this work
LT1865	MG1655 *ΔlacI-kan luc-N pLoL rexB<>cat rexA*$^+$ *cI857ind1 pRoR cro27 cII-lacZYA*	this work
LT1866	MG1655 *ΔlacI-kan luc-N pLoL (rexB-rexA<>cat) cI857ind1 pRoR cro27 cII-lacZYA*	this work
LT1886	MG1655 *ΔlacI-kan luc-N pLoL rexB*$^+$ *rexA*$^+$ *cI857 pRoR cro*$^+$ *cII-lacZYA*	this work
LT1887	MG1655 *ΔlacI-kan luc-N pLoL rexB*$^+$ *rexA<>cat cI857ind1 pRoR cro*$^+$ *cII-lacZYA*	this work
LT1891	MG1655 *ΔlacI-kan luc-N pLoL rexB<>cat rexA*$^+$ *cI857ind1 pRoR cro*$^+$ *cII-lacZYA*	this work
LT1892	MG1655 *ΔlacI-kan luc-N pLoL (rexB-rexA<>cat) cI857ind1 pRoR cro*$^+$ *cII-lacZYA*	this work
LT1895	MG1655 *ΔlacI-kan luc-N pLoL rexB<>cat rexA*$^+$ *cI*$^+$ *pRoR cro*$^+$ *cII-lacZYA*	
LT1897	*MG1655 ΔlacI-kan luc-N pLoL (rexB-rexA<>cat) cI*$^+$ *pRoR cro*$^+$ *cII-lacZYA*	
LT2063	LT1886 *Δ (srlA- recA)::*Tn*10*	this work

LT2064	LT1887 *Δ (srlA- recA)::*Tn*10*	this work
LT2065	LT1891 *Δ (srlA- recA)::*Tn*10*	this work
LT2066	LT1892 *Δ (srlA- recA)::*Tn*10*	this work
LT2109	LT1678 P_{BAD}-(*rexA*$^{+}$ *rexB)*$^{+}$	this work
LT2319	MG1655(λ *cI857 ind1 rexB*$^{+}$*rexA<>cat*) *lamB<>kan* monolysogen	this work
LT2320	MG1655(λ *cI857 ind1 rexB<>cat rexA*$^{+}$) *lamB<>kan* monolysogen	this work
LT2321	MG1655(λ *cI857 ind1(rexB rexA)<>cat*) *lamB<>kan* monolysogen	this work

669

Table 2. β-galactosidase measurements for BACTH system demonstrates protein-protein interaction between RexA and RexB with CI and Cro repressors[†]

Strain Number	Relevant Genotype	Configurations of hybrid proteins	β-galactosidase Units[‡]
LT2333	BTH101[pKT25-*rexA*] [pUT18C-*c*I]	*cya25-rexA* *cya18-c*I	86 ± 20 (n=9)
LT2381	BTH101[pKT25-*c*I] [pUT18C-*rexA*]	*cya25-c*I *cya18-rexA*	105 ± 28 (n=9)
LT2447	LT2333 *nadA::Tn*10 (λ*c*I<>*kan Δ(N-int)*)	*cya25-rexA* *cya18-c*I	94 ± 6 (n=6)
LT2388	BTH101[pKT25-*cro*] [pUT18C-*rexA*]	*cya25-cro* *cya18-rexA*	55 ± 1.2 (n=6)
LT2331	BTH101[pKT25-*rexB*] [pUT18C-*c*I]	*cya25-rexB* *cya18-c*I	558± 129 (n=9)
LT2332	BTH101[pKNT25-*rexB*] [pUT18C-*c*I]	*rexB-cya25* *cya18-c*I	252 ± 74 (n=9)
LT2383	BTH101[pKT25-*c*I] [pUT18-*rexB*]	*cya25-c*I *rexB-cya18*	118 ± 30 (n=6)
LT2385	BTH101[pKT25-*c*I] [pUT18C-*rexB*]	*cya25-c*I *cya18-rexB*	104 ± 17 (n=6)
LT2446	LT2331 *nadA::Tn*10 (λ*c*I<>*kan Δ(N-int)*)	*cya25-rexB* *cya18-c*I	247 ± 125 (n=6)

LT2394	BTH101[pKT25-*cro*] [pUT18C-*rexB*]	*cya25-cro* *cya18-rexB*	316 ± 138 (n=6)
LT2410	BTH101[pKT25-*cro*] [pUT18C-*c*I]	*cya25-cro* *cya18-c*I	84 ± 18 (n=6)
LT2415	BTH101[pKT25-*c*I] [pUT18C-*c*I]	*cya25-c*I *cya18-c*I	893 ± 46 (n=5)
LT2416	BTH101[pKT25-*cro*] [pUT18C-*cro*]	*cya25-cro* *cya18-cro*	631 ± 173 (n=5)

[†]Only plasmid pairs conferring growth on minimal maltose are included here.
[‡]Standard error of the mean is shown.

676 **References**

677

678 Arkin, A., Ross, J., & McAdams, H. H. (1998). Stochastic kinetic analysis of developmental
679 pathway bifurcation in phage lambda-infected Escherichia coli cells. *Genetics, 149*(4),
680 1633-1648.
681 Baek, K., Svenningsen, S., Eisen, H., Sneppen, K., & Brown, S. (2003). Single-cell analysis of λ
682 immunity regulation. *J Mol Biol, 334*(3), 363-372.
683 Beckett, D., Burz, D. S., Ackers, G. K., & Sauer, R. T. (1993). Isolation of λ repressor mutants
684 with defects in cooperative operator binding. *Biochemistry, 32*(35), 9073-9079.
685 doi:10.1021/bi00086a012
686 Bednarz, M., Halliday, J. A., Herman, C., & Golding, I. (2014). Revisiting bistability in the
687 lysis/lysogeny circuit of bacteriophage lambda. *PLoS One, 9*(6), e100876.
688 doi:10.1371/journal.pone.0100876
689 Bell, C. E., Frescura, P., Hochschild, A., & Lewis, M. (2000). Crystal structure of the lambda
690 repressor C-terminal domain provides a model for cooperative operator binding. *Cell,*
691 *101*(7), 801-811. doi:10.1016/s0092-8674(00)80891-0
692 Benzer, S. (1955). FINE STRUCTURE OF A GENETIC REGION IN BACTERIOPHAGE.
693 *Proc Natl Acad Sci U S A, 41*(6), 344-354.
694 Burz, D. S., & Ackers, G. K. (1994). Single-site mutations in the C-terminal domain of
695 bacteriophage λ *c*I repressor alter cooperative interactions between dimers adjacently
696 bound to O_R. *Biochemistry, 33*(28), 8406-8416. doi:10.1021/bi00194a004
697 Coetzee, W. F., & Pollard, E. C. (1974). Near-UV effects on the induction of prophage. *Radiat*
698 *Res, 57*(2), 319-331.

699 Craig, N. L., & Roberts, J. W. (1980). *E. coli* recA protein-directed cleavage of phage λ repressor
700 requires polynucleotide. *Nature, 283*(5742), 26-30. doi:10.1038/283026a0
701 Crick, F. H., Barnett, L., Brenner, S., & Watts-Tobin, R. J. (1961). General nature of the genetic
702 code for proteins. *Nature, 192*, 1227-1232. doi:10.1038/1921227a0
703 d'Ari, R. (1985). The SOS system. *Biochimie, 67*(3-4), 343-347. doi:10.1016/s0300-
704 9084(85)80077-8
705 Darling, P. J., Holt, J. M., & Ackers, G. K. (2000). Coupled energetics of λ *cro* repressor self-
706 assembly and site-specific DNA operator binding II: cooperative interactions of *cro*
707 dimers. *J Mol Biol, 302*(3), 625-638. doi:10.1006/jmbi.2000.4050
708 Dodd, I. B., Perkins, A. J., Tsemitsidis, D., & Egan, J. B. (2001). Octamerization of lambda CI
709 repressor is needed for effective repression of P(RM) and efficient switching from
710 lysogeny. *Genes Dev, 15*(22), 3013-3022. doi:10.1101/gad.937301
711 Dodd, I. B., Shearwin, K. E., & Egan, J. B. (2005). Revisited gene regulation in bacteriophage λ.
712 *Curr Opin Genet Dev, 15*(2), 145-152. doi:10.1016/j.gde.2005.02.001
713 Echols, H. (1986). Bacteriophage λ development: temporal switches and the choice of lysis or
714 lysogeny. *Trends in Genetics, 2*, 26-30.
715 Echols, H., Green, L., Oppenheim, A. B., Oppenheim, A., & Honigman, A. (1973). Role of the
716 *cro* gene in bacteriophage λ development. *J Mol Biol, 80*(2), 203-216. doi:10.1016/0022-
717 2836(73)90167-8
718 Eisen, H., Brachet, P., Pereira da Silva, L., & Jacob, F. (1970). Regulation of repressor
719 expression in λ. *Proc Natl Acad Sci U S A, 66*(3), 855-862. doi:10.1073/pnas.66.3.855
720 Eisen, H., Georgiou, M., Georgopoulos, C. P., Selzer, G., Gussin, G., & Herskowitz, I. (1975).
721 The role of gene *cro* in phage development. *Virology, 68*(1), 266-269.

722 Ennis, D. G., Ossanna, N., & Mount, D. W. (1989). Genetic separation of *Escherichia coli recA*
723 functions for SOS mutagenesis and repressor cleavage. *J Bacteriol, 171*(5), 2533-2541.
724 doi:10.1128/jb.171.5.2533-2541.1989
725 Folkmanis, A., Maltzman, W., Mellon, P., Skalka, A., & Echols, H. (1977). The essential role of
726 the *cro* gene in lytic development by bacteriophage λ. *Virology, 81*(2), 352-362.
727 doi:10.1016/0042-6822(77)90151-9
728 Gentile, G. M., Wetzel, K. S., Dedrick, R. M., Montgomery, M. T., Garlena, R. A., Jacobs-Sera,
729 D., & Hatfull, G. F. (2019). More Evidence of Collusion: a New Prophage-Mediated
730 Viral Defense System Encoded by Mycobacteriophage Sbash. *MBio, 10*(2).
731 doi:10.1128/mBio.00196-19
732 Gimble, F. S., & Sauer, R. T. (1985). Mutations in bacteriophage λ repressor that prevent RecA-
733 mediated cleavage. *J Bacteriol, 162*(1), 147-154.
734 Golding, I. (2011). Decision making in living cells: lessons from a simple system. *Annu Rev*
735 *Biophys, 40*, 63-80. doi:10.1146/annurev-biophys-042910-155227
736 Golding, I. (2016). Single-Cell Studies of Phage λ: Hidden Treasures Under Occam's Rug. *Annu*
737 *Rev Virol, 3*(1), 453-472. doi:10.1146/annurev-virology-110615-042127
738 Gussin, G. N., & Peterson, V. (1972). Isolation and properties of rex$^-$ mutants of bacteriophage
739 lambda. *J Virol, 10*(4), 760-765. doi:10.1128/jvi.10.4.760-765.1972
740 Hallick, L. M., & Echols, H. (1973). Genetic and biochemical properties of an association
741 complex between host components and lambda DNA. *Virology, 52*(1), 105-119.
742 doi:10.1016/0042-6822(73)90402-9

743 Hayes, S., Bull, H. J., & Tulloch, J. (1997). The Rex phenotype of altruistic cell death following
744 infection of a λ lysogen by T4*rII* mutants is suppressed by plasmids expressing OOP
745 RNA. *Gene, 189*(1), 35-42.
746 Hayes, S., & Szybalski, W. (1973). Control of short leftward transcripts from the immunity and
747 *ori* regions in induced coliphage lambda. *Mol Gen Genet, 126*(4), 275-290.
748 Jacob, F., & Campbell, A. (1959). [System of repression insuring immunity in lysogenic
749 bacteria]. *C R Hebd Seances Acad Sci, 248*(22), 3219-3221.
750 Johnson, A., Meyer, B. J., & Ptashne, M. (1978). Mechanism of action of the *cro* protein of
751 bacteriophage λ. *Proc Natl Acad Sci U S A, 75*(4), 1783-1787.
752 doi:10.1073/pnas.75.4.1783
753 Johnson, A. D., Meyer, B. J., & Ptashne, M. (1979). Interactions between DNA-bound repressors
754 govern regulation by the λ phage repressor. *Proc Natl Acad Sci U S A, 76*(10), 5061-
755 5065.
756 Karimova, G., Gauliard, E., Davi, M., Ouellette, S. P., & Ladant, D. (2017). Protein-Protein
757 Interaction: Bacterial Two-Hybrid. *Methods Mol Biol, 1615*, 159-176. doi:10.1007/978-
758 1-4939-7033-9_13
759 Krogh, A., Larsson, B., von Heijne, G., & Sonnhammer, E. L. (2001). Predicting transmembrane
760 protein topology with a hidden Markov model: application to complete genomes. *J Mol*
761 *Biol, 305*(3), 567-580. doi:10.1006/jmbi.2000.4315
762 Landsmann, J., Kroger, M., & Hobom, G. (1982). The *rex* region of bacteriophage lambda: two
763 genes under three-way control. *Gene, 20*(1), 11-24.

764 Lee, S., Lewis, D. E. A., & Adhya, S. (2018). The Developmental Switch in Bacteriophage λ: A
765 Critical Role of the Cro Protein. *J Mol Biol, 430*(1), 58-68.
766 doi:10.1016/j.jmb.2017.11.005
767 Lewis, D. E. A., Gussin, G. N., & Adhya, S. (2016). New Insights into the Phage Genetic
768 Switch: Effects of Bacteriophage Lambda Operator Mutations on DNA Looping and
769 Regulation of P_R, P_L, and P_{RM}. *J Mol Biol, 428*(22), 4438-4456.
770 doi:10.1016/j.jmb.2016.08.027
771 Little, J. W., & Michalowski, C. B. (2010). Stability and instability in the lysogenic state of
772 phage lambda. *J Bacteriol, 192*(22), 6064-6076. doi:10.1128/jb.00726-10
773 Liu, X., Jiang, H., Gu, Z., & Roberts, J. W. (2013). High-resolution view of bacteriophage
774 lambda gene expression by ribosome profiling. *Proc Natl Acad Sci U S A, 110*(29),
775 11928-11933. doi:10.1073/pnas.1309739110
776 MacHattie, L. A. (1985). Endpoint distribution for deletions into *imm*λ region forming pλCM
777 replicons: phage λ gene *rex* affects plasmid establishment. *Gene, 37*(1-3), 19-30.
778 doi:10.1016/0378-1119(85)90253-7
779 Mageeney, C. M., Mohammed, H. T., Dies, M., Anbari, S., Cudkevich, N., Chen, Y., . . . Ware,
780 V. C. (2020). Mycobacterium Phage Butters-Encoded Proteins Contribute to Host
781 Defense against Viral Attack. *mSystems, 5*(5). doi:10.1128/mSystems.00534-20
782 Maniatis, T., & Ptashne, M. (1973). Multiple repressor binding at the operators in bacteriophage
783 λ. *Proc Natl Acad Sci U S A, 70*(5), 1531-1535. doi:10.1073/pnas.70.5.1531
784 Matz, K., Schmandt, M., & Gussin, G. N. (1982). The *rex* gene of bacteriophage λ is really two
785 genes. *Genetics, 102*(3), 319-327.

786 Montgomery, M. T., Guerrero Bustamante, C. A., Dedrick, R. M., Jacobs-Sera, D., & Hatfull, G.
787 F. (2019). Yet More Evidence of Collusion: a New Viral Defense System Encoded by
788 Gordonia Phage CarolAnn. *MBio, 10*(2). doi:10.1128/mBio.02417-18
789 Oppenheim, A. B., Kobiler, O., Stavans, J., Court, D. L., & Adhya, S. (2005). Switches in
790 bacteriophage lambda development. *Annu Rev Genet, 39*, 409-429.
791 doi:10.1146/annurev.genet.39.073003.113656
792 Ouellette, S. P., Karimova, G., Davi, M., & Ladant, D. (2017). Analysis of Membrane Protein
793 Interactions with a Bacterial Adenylate Cyclase-Based Two-Hybrid (BACTH)
794 Technique. *Curr Protoc Mol Biol, 118*, 20.12.21-20.12.24. doi:10.1002/cpmb.36
795 Parma, D. H., Snyder, M., Sobolevski, S., Nawroz, M., Brody, E., & Gold, L. (1992). The Rex
796 system of bacteriophage λ: tolerance and altruistic cell death. *Genes Dev, 6*(3), 497-510.
797 Powell, B. S., Rivas, M. P., Court, D. L., Nakamura, Y., & Turnbough, C. L., Jr. (1994). Rapid
798 confirmation of single copy lambda prophage integration by PCR. *Nucleic Acids Res,*
799 *22*(25), 5765-5766. doi:10.1093/nar/22.25.5765
800 Ptashne, M., & Hopkins, N. (1968). The operators controlled by the λ phage repressor. *Proc Natl*
801 *Acad Sci U S A, 60*(4), 1282-1287.
802 Ptashne, M., Jeffrey, A., Johnson, A. D., Maurer, R., Meyer, B. J., Pabo, C. O., . . . Sauer, R. T.
803 (1980). How the λ repressor and Cro work. *Cell, 19*(1), 1-11.
804 Raibaud, O., Vidal-Ingigliardi, D., & Kolb, A. (1991). Genetic studies on the promoter of *malT*,
805 the gene that encodes the activator of the *Escherichia coli* maltose regulon. *Res*
806 *Microbiol, 142*(9), 937-942. doi:10.1016/0923-2508(91)90003-s

807 Reichardt, L. F. (1975). Control of bacteriophage lambda repressor synthesis: regulation of the
808 maintenance pathway of the *cro* and *cI* products. *J Mol Biol, 93*(2), 289-309.
809 doi:10.1016/0022-2836(75)90133-3
810 Révet, B., von Wilcken-Bergmann, B., Bessert, H., Barker, A., & Müller-Hill, B. (1999). Four
811 dimers of lambda repressor bound to two suitably spaced pairs of lambda operators form
812 octamers and DNA loops over large distances. *Curr Biol, 9*(3), 151-154.
813 doi:10.1016/s0960-9822(99)80069-4
814 Russell, D. A., & Hatfull, G. F. (2017). PhagesDB: the actinobacteriophage database.
815 *Bioinformatics, 33*(5), 784-786. doi:10.1093/bioinformatics/btw711
816 Schoulaker-Schwarz, R., Dekel-Gorodetsky, L., & Engelberg-Kulka, H. (1991). An additional
817 function for bacteriophage λ *rex*: the rexB product prevents degradation of the λ O
818 protein. *Proc Natl Acad Sci U S A, 88*(11), 4996-5000.
819 Snyder, L., & McWilliams, K. (1989). The *rex* genes of bacteriophage lambda can inhibit cell
820 function without phage superinfection. *Gene, 81*(1), 17-24.
821 Spiegelman, W. G., Reichardt, L. F., Yaniv, M., Heinemann, S. F., Kaiser, A. D., & Eisen, H.
822 (1972). Bidirectional transcription and the regulation of Phage λ repressor synthesis. *Proc*
823 *Natl Acad Sci U S A, 69*(11), 3156-3160. doi:10.1073/pnas.69.11.3156
824 Stayrook, S., Jaru-Ampornpan, P., Ni, J., Hochschild, A., & Lewis, M. (2008). Crystal structure
825 of the λ repressor and a model for pairwise cooperative operator binding. *Nature,*
826 *452*(7190), 1022-1025. doi:10.1038/nature06831
827 Sussman, R., & Jacob, F. (1962). [On a thermosensitive repression system in the Escherichia coli
828 lambda bacteriophage]. *C R Hebd Seances Acad Sci, 254*, 1517-1519.

Svenningsen, S. L., Costantino, N., Court, D. L., & Adhya, S. (2005). On the role of Cro in λ prophage induction. *Proc Natl Acad Sci U S A, 102*(12), 4465-4469. doi:0409839102 [pii] 10.1073/pnas.0409839102

Thomason, L. C., Costantino, N., & Court, D. L. (2007). *E. coli* genome manipulation by P1 transduction. *Curr Protoc Mol Biol, Chapter 1*, Unit 1 17. doi:10.1002/0471142727.mb0117s79

Thomason, L. C., Morrill, K., Murray, G., Court, C., Shafer, B., Schneider, T. D., & Court, D. L. (2019). Elements in the λ immunity region regulate phage development: beyond the 'Genetic Switch'. *Mol Microbiol, 112*(6), 1798-1813. doi:10.1111/mmi.14394

Thomason, L. C., Sawitzke, J. A., Li, X., Costantino, N., & Court, D. L. (2014). Recombineering: genetic engineering in bacteria using homologous recombination. *Curr Protoc Mol Biol, 106*, 1.16.11-39. doi:10.1002/0471142727.mb0116s106

Toothman, P., & Herskowitz, I. (1980). Rex-dependent exclusion of lambdoid phages. I. Prophage requirements for exclusion. *Virology, 102*(1), 133-146.

Whipple, F. W., Kuldell, N. H., Cheatham, L. A., & Hochschild, A. (1994). Specificity determinants for the interaction of λ repressor and P22 repressor dimers. *Genes Dev, 8*(10), 1212-1223. doi:10.1101/gad.8.10.1212

Witkin, E. M. (1991). RecA protein in the SOS response: milestones and mysteries. *Biochimie, 73*(2-3), 133-141. doi:10.1016/0300-9084(91)90196-8

Figure Legends

Figure 1. Genetic map of λ immunity region and DNA replication genes. The CI and Cro repressors are expressed in the P_{RM} and P_R operons, respectively, and are major players in the lysis-lysogeny decision. These two repressors control expression of the major lytic promoters P_L and P_R by binding to the left and right tripartite operator sites, O_L and O_R, with the lytic P_R and lysogenic P_{RM} promoters sharing coordinate but opposing regulation within the O_R segment. The *rexA* and *rexB* genes are downstream of *c*I. The P_{LIT} promoter is embedded in the terminal coding sequence of *rexA*, with the consequence that *rexB* is transcribed from two promoters, P_{RM} and P_{LIT}, while *c*I and *rexA* are transcribed only from P_{RM} (Thomason et al 2019). Black arrows represent the beginning of the various promoter transcripts shown. Transcription from P_{RM} and P_{LIT} ends at the transcriptional terminator, T_{IMM}, immediately downstream of *rexB*. The DNA replication genes *O* and *P* are transcribed from P_R, as is *ren*, which is also likely involved in DNA replication.

Figure 2. RexA$^+$ enhances UV induction of a λ *c*I$^+$ prophage at low UV doses. UV induction of λ lysogens was performed as described in Experimental Procedures. **A.** LT445 is MG1655(λ *c*I$^+$ *rexA*$^+$ *rexB*$^+$) (●) (n=7); LT1676 is MG1655(λ*c*I$^+$ *rexA*<>*cat rexB*$^+$) (Δ) (n=3); LT1677 is MG1655(λ*c*I$^+$ *rexA*$^+$ *rexB*<>*cat*) (▲) (n=6), LT1678 is MG1655(λ*c*I$^+$ *rexA-rexB*<>*cat*) (○) (n=3). Titers of the lysates on strain A584 were determined at t=0 and the time points indicated following UV irradiation. **B.** LT445 is MG1655(λ) (●); LT1678 is MG1655(λ *rexA-rexB*<>*cat*) (○) (n=3); LT2109 is MG1655(λ *rexA-rexB*<>*cat*)/P_{BAD}-*rexA*$^+$ *rexB*$^+$ (□) (n=4). Data have been analyzed by the standard error of the mean (s.e.m). The number of trials is indicated by (n).

872

873 **Figure 3. Genetic map of dual P_L P_R reporter.** The phage λ immunity region has been inserted
874 within the *E. coli lac* operon such that expression of *lacZ* is driven from the P_R lytic promoter
875 (Svenningsen 2005) with the *lacI* gene and the *lac* promoter being replaced by P_R. This leaves
876 the *lacZ* ribosome-binding site and the rest of the *lacZYA* operon intact. Versions of this reporter
877 with the temperature sensitive *cI857* repressor were used to determine the effects of RexA and/or
878 RexB functions on induction and the switch to activate P_L and P_R promoter transcription. Single
879 colonies were grown on MacConkey Lactose indicator medium. When the switch is in the CI-
880 repressed or immune state, colonies do not express LacZ and are white. When the switch is in the
881 Cro-repressed nonimmune state, *lacZ* is expressed from P_R and the colonies are red. The firefly
882 luciferase gene *luc* replaces the λ *N* gene beyond the P_L promoter.

883

884 **Figure 4. RexA promotes the transition to nonimmune state within individual colonies.** In
885 these pictures, colonies of strains containing the P_L and P_R reporters with the temperature
886 sensitive *cI857* repressor allele were plated on MacConkey Lactose agar and incubated at 32º-
887 34ºC. All colonies are white after one day of incubation but develop red papillae after two days,
888 indicative of a transition to the lytic state by cells within the colony and consequent expression of
889 *lacZ* from P_R. The *rex* genotypes are indicated, and the strain numbers are shown below. **A.** Top
890 row: the strains (LT1886, LT1887, LT1891, and LT1892) display different papillation levels
891 dependent on the genotype of the *rexA* and *rexB* genes. **B.** Middle row: The *recA* mutant strains
892 (LT2063, LT2064, LT2065, and LT2066) also display variable papillation based on *rex*
893 genotype. **C.** Bottom row: The *cro27* mutant strains of λ (LT1055, LT1395, LT1865, and
894 LT1866) all papillate similarly, regardless of *rex* genotype.

Figure 5. RexA function stabilizes the non-immune state. $RecA^+$ and $RecA^-$ colonies containing the Cro^+ P_R reporter pictured in Fig. 3 were analyzed to determine the effect of RexA and RexB on the frequency of returning from the non-immune state to the immune state in the presence of Cro repression. The y-axis indicates the percentage of immune (white) colonies arising during overnight growth of a culture that initially carried a reporter in the non-immune (red) state. The final number of colonies analyzed for each genotype is indicated. The error bars show the standard deviation (s.d.). **A.** $RecA^+$ strains: LT1886, *rexA*$^+$ *rexB*$^+$(n=18); LT1887, *rexA*$^-$ *rexB*$^+$ (n=21); LT1891, *rexA*$^+$ *rexB*$^-$ (n=22); LT1892, *rexA*$^-$ *rexB*$^-$ (n=20). **B.** *ΔrecA* strains: LT2063, *rexA*$^+$ *rexB*$^+$ (n=17); LT2064, *rexA*$^-$ *rexB*$^+$ (n=14); LT2065, *rexA*$^+$ *rexB*$^-$ (n=15); LT2066, *rexA*$^-$ *rexB*$^-$ (n=14).

Figure 6. Monitoring luciferase activity from P_L *N-luc* after inducing DNA damage. After addition of Mitomycin C, expression of firefly luciferase from the P_L promoter (P_L *N-luc*) was monitored over time for four strains carrying the lambda immunity region and different *rexA* and *rexB* mutations. Relative light units are shown on the y-axis and time in minutes on the x-axis. The DNA damage inducer, Mitomycin C, was added at t=0. For the first ~two hours all points are congruent, but Rex-dependent genotypic differences arise in luciferase expression are apparent after ~150 min. (A). LT1895, *rexA*$^+$ *rexB*<>*cat* (Δ) vs. LT1897, (*rexA rexB*)<>*cat* (○). (B). LT1659, *rexA*<>*cat rexB*$^+$ (▲) vs. LT1897, (*rexA rexB*)<>*cat* (○).(C). LT1895, *rexA*$^+$ *rexB*<>*cat* (Δ) vs. LT1657, *rexA*$^+$ *rexB*$^+$ (●). (D). LT1659, *rexA*<>*cat rexB*$^+$ (▲) vs. LT1657, *rexA*$^+$ *rexB*$^+$ (●). (E). LT1657, *rexA*$^+$ *rexB*$^+$ (●) vs. LT1897, (*rexA rexB*)<>*cat* (○). The

experiment was repeated three times with duplicate technical replicates each time; one representative experiment is shown.

Figure 7. RexA and RexB affect the level of spontaneous phage release from λ*cI857 ind1* lysogens. The bar graph shows the plaque-forming units (PFU) per ml of spontaneously released phage particles arising during 32°C growth of lysogenic cultures. Strain numbers and *rex* genotypes for each culture are indicated below the bars. Three independent repetitions of each experiment were performed; error bars represent the standard deviation (s.d.).

Figure 8. RexA forms stable complexes with CI and DNA *in vitro*. A. SEC-MALS analysis of purified RexA. UV trace (black) and measured mass based on light scattering (blue) are shown. **B.** SEC analysis of RexA and CI protein-protein and protein-DNA interactions. SDS-PAGE gels (silver-stained for DNA and Coomassie-stained for protein) from individual SEC injections are numbered with Roman numerals and shown to visualize shifts in retention volume off of SEC in response to different conditions. Molecular weight standards in kDa are shown in the first lane of each gel with samples labeled on the right. All samples were run on a Superdex 200 PC 3.2 column (GE). The elution volume across the fractions is marked above along with the relative positions of molecular weight standards (F, ferritin, 440 kDa; A, aldolase, 158 kDa; C, conalbumin, 75 kDa; O, ovalbumin, 44 kDa; CA, carbonic anhydrase, 29 kDa). A leftward shift of the bands indicates formation of a larger molecular weight species and is associated with complex formation. See Materials and Methods and Table S3 for DNA substrate preparation and oligonucleotide sequences, respectively. **C.** Filter binding analysis of RexA interactions with different DNA substrates. Substrate nomenclature: OR1-OR2, double-stranded DNA containing

940 wildtype O_R1 and O_R2 operator sites; ss, single-stranded DNA; scrambled, mutated substrate
941 altering operator site sequences. Binding was performed with wildtype RexA at 30°C for 10 min
942 in a 30 µL reaction mixture containing 14.5 nM unlabeled DNA and 0.5 nM labelled DNA.
943 Samples were filtered through KOH-treated nitrocellulose and binding was assessed by
944 scintillation counting. The data points represent the averages of at least three independent
945 experiments (mean ± standard deviation) and were compared to a negative control to determine
946 fraction bound.
947
948 **Figure 9. Effect of RexA on the transition from the lytic state to the immune state.** When
949 only the phage immunity region is present on the *E. coli* chromosome (see Figure 3), the bistable
950 switch can be in either the immune or nonimmune state. The purified red colonies used for the
951 experiment of Figure 5 have the switch in the nonimmune state, with the Cro protein expressed
952 from P_R repressing P_{RM}, so that cI and *rexA* are not expressed. Because of stochastic events,
953 switching to the immune state may occur that relieves Cro repression and allows some P_{RM}
954 transcription, resulting in *c*I and *rexA* expression. The data of Figure 5 show that in this situation,
955 RexA protein lessens the probability that CI can establish immune repression, and thus RexA
956 stabilizes the lytic state. If *rexA* is mutant, the switch tends to return to the lysogenic state.
957
958 **Figure 10. Model for involvement of RexA and RexB in the transition to lytic growth.**
959 **Top Panel:** The divergent P_{RM} and P_R promoters and the right operator sites are illustrated. In
960 the lysogenic state, CI dimers are bound cooperatively to O_{R1} and O_{R2}, repressing P_R, and
961 transcription of P_{RM} is activated by CI contacting RNA polymerase. Similar CI dimers bound to
962 O_{L1} and O_{L2} repress the P_L promoter (not shown in diagram), with long-range DNA looping

963 between the left and right operators mediated by CI repressor molecules. This is the normal state
964 in a λ lysogen. In response to an inducing signal such as DNA damage, RecA protein becomes
965 activated (RecA*) and binds to CI repressor, promoting CI inactivation. This allows transcription
966 from P_L and P_R and subsequent Cro expression; Cro will bind to O_{R3} and repress P_{RM}
967 transcription. **Middle Panel:** Our two-hybrid data suggest protein-protein interactions between
968 CI repressor and the integral membrane protein, RexB. Here, we have shown the CI repressor
969 protein bound to the operator sites while in association with RexB, which may prevent RexA
970 action and deepen repression. This postulated membrane association is not the tight membrane
971 tethering of the lambda genome observed by Hallick and Echols (1973). Our two-hybrid data
972 also show interaction between RexB and RexA (Thomason et al. 2019). **Bottom Panel:** It is
973 possible that CI, RexB, and RexA co-localize at the periphery of the inner membrane to form a
974 complex that includes all three proteins. CI and RexA can be released from RexB, perhaps in
975 response to an environmental signal or a conformational change in RexB. RexA is then free to
976 interact with CI repressor bound to DNA at the operator sites; RexA may also bind DNA
977 nonspecifically. These protein-protein and protein-DNA interactions may destabilize CI
978 repression and activate the lytic state.
979
980 **Figure 11. Predicted RexB membrane topology and location of charged amino acid**
981 **residues.** The computer program TMHMM was used to predict the orientation of RexB in the *E.*
982 *coli* cytoplasmic membrane. The numbers indicate the locations of amino acid residues, with the
983 first and last residues of each transmembrane spanning domain shown. The negatively charged
984 residue in the third transmembrane domain may serve as a proton sink and play some role in

985 energetics. The relative locations of charged amino acids are also indicated. Created with

986 BioRender.com.

987

Figure 1

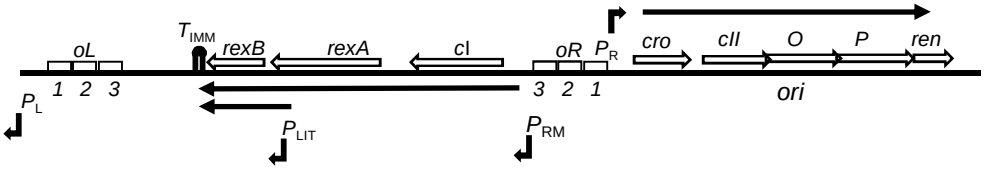

Figure 2

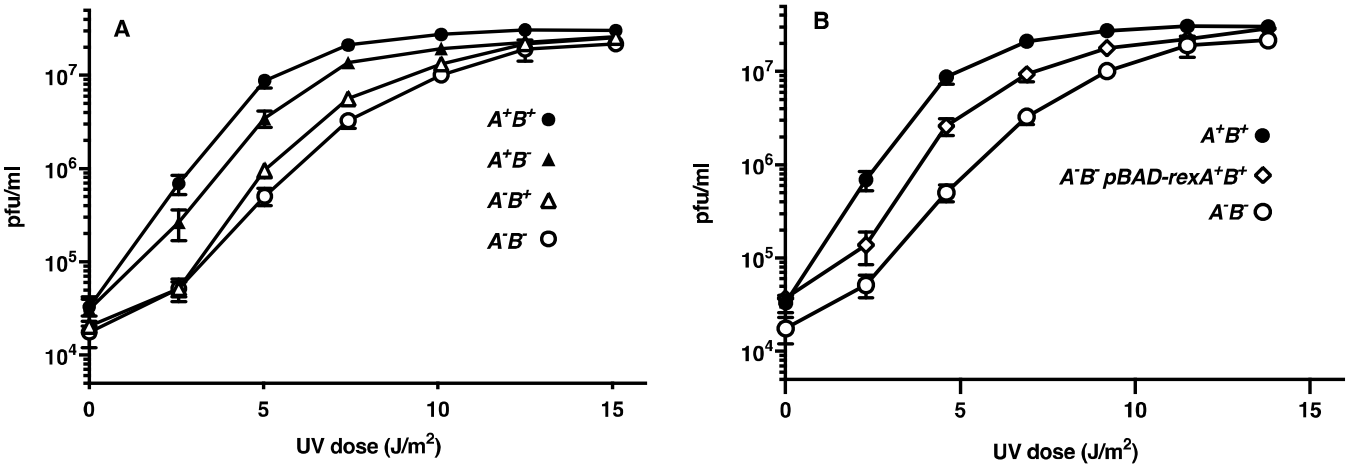

Figure 3

A.

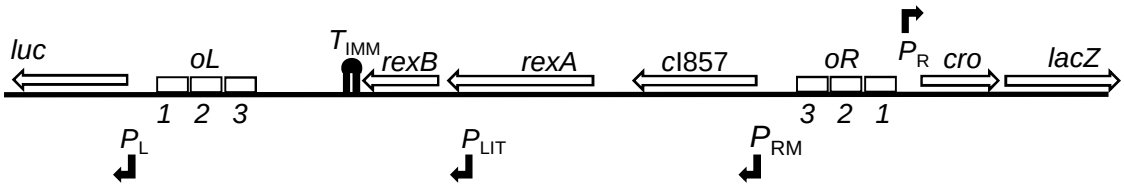

Figure 4

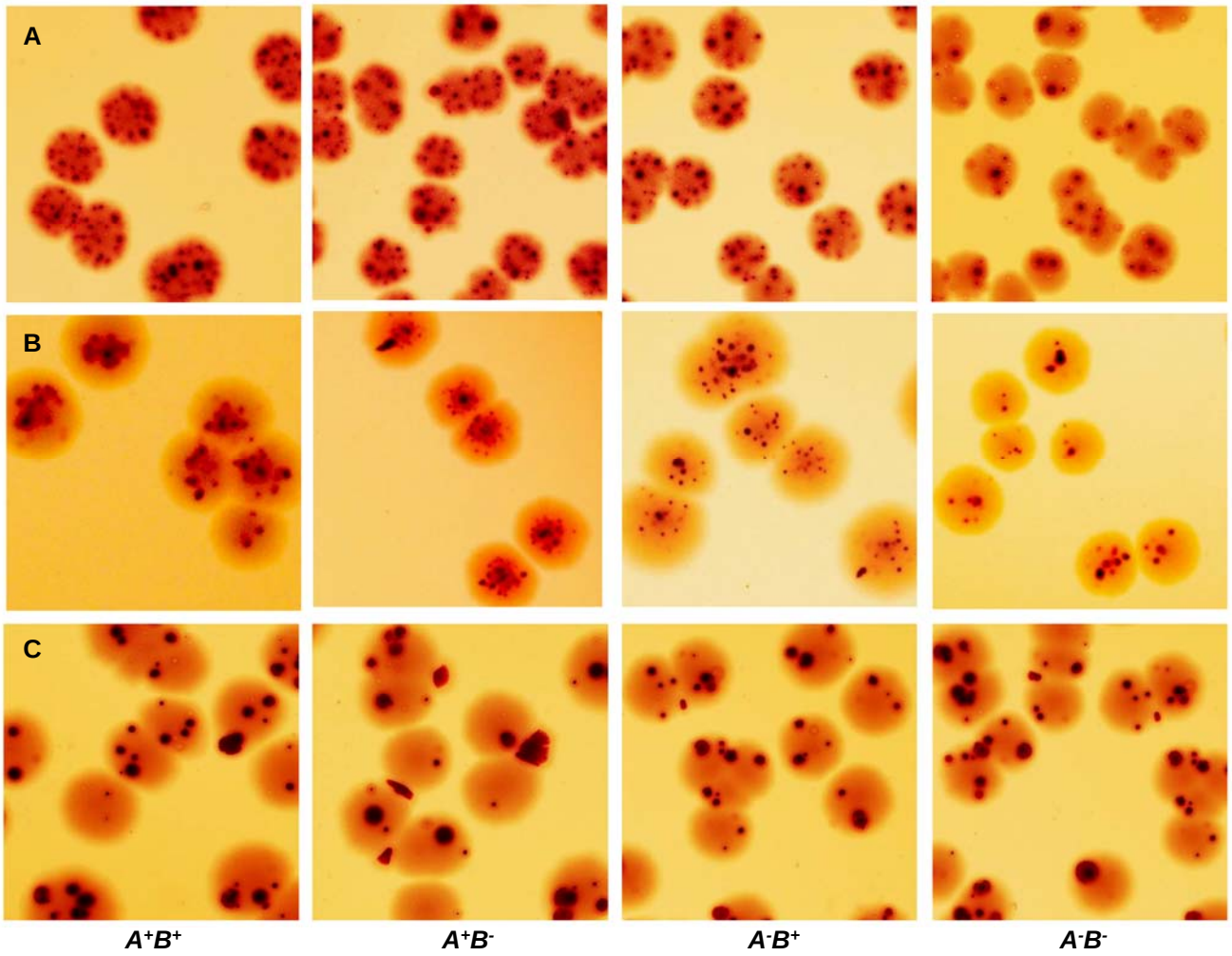

Figure 5.

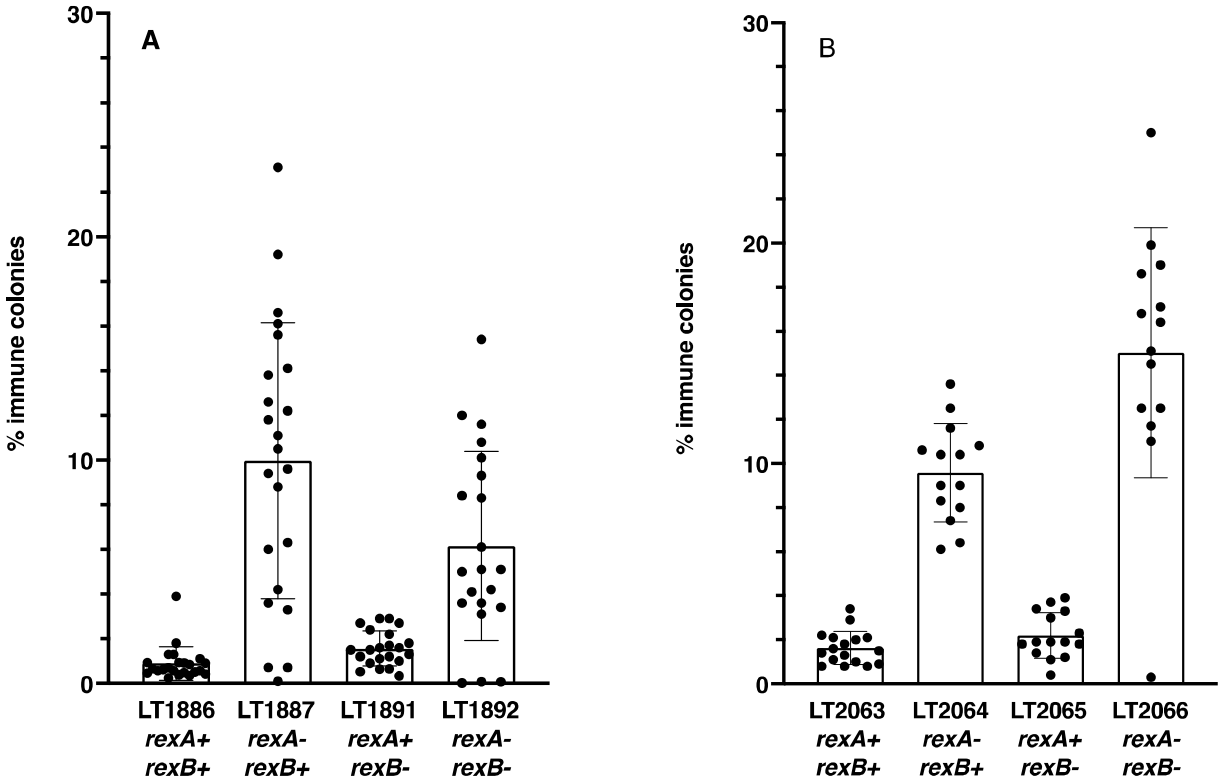

Figure 6.

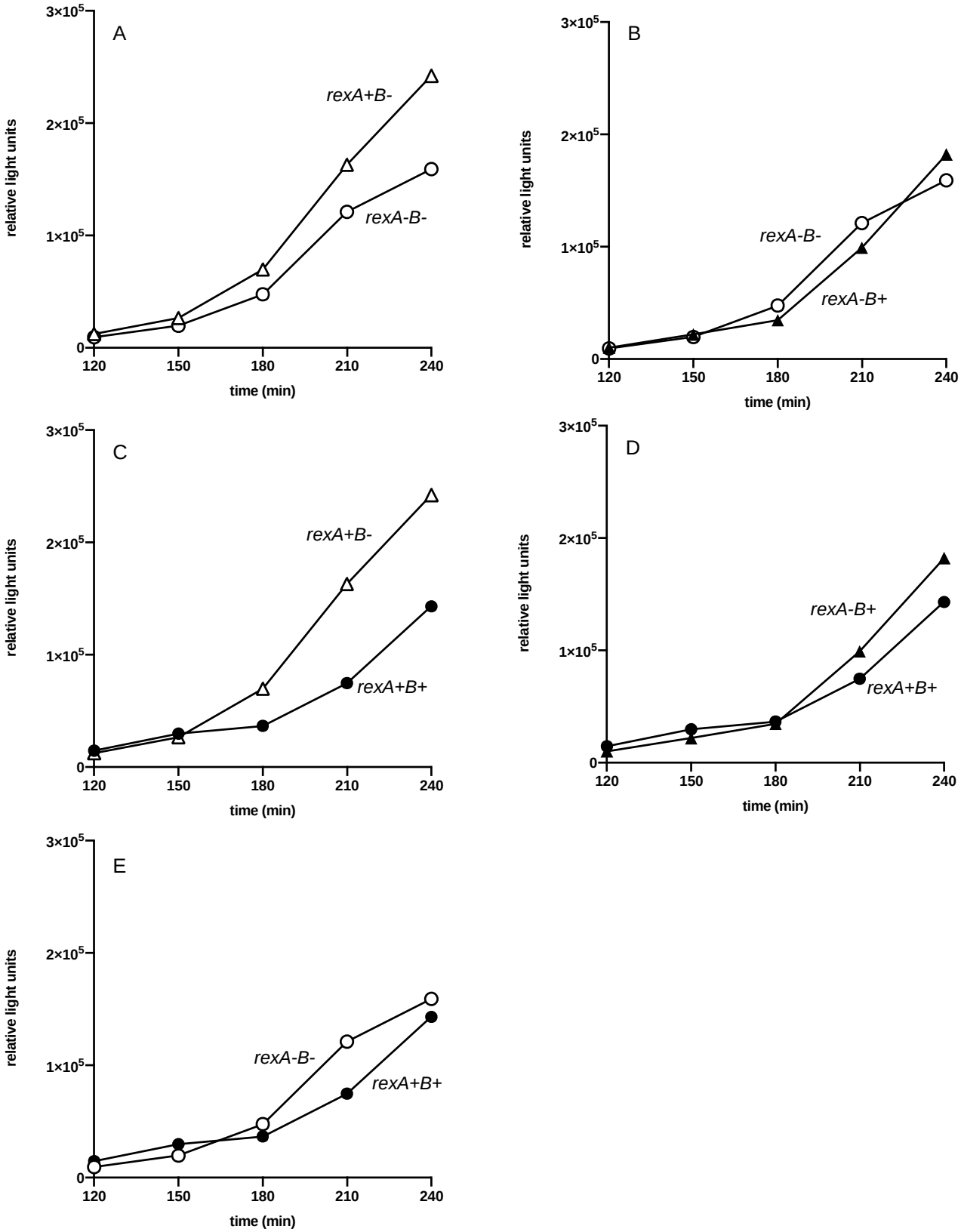

Figure 7.

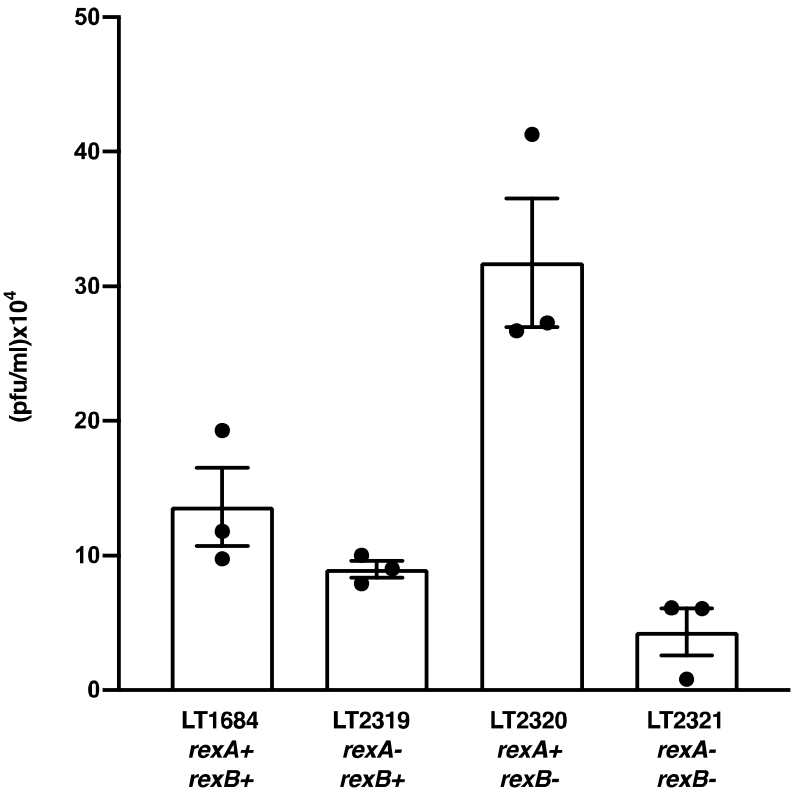

Figure 8

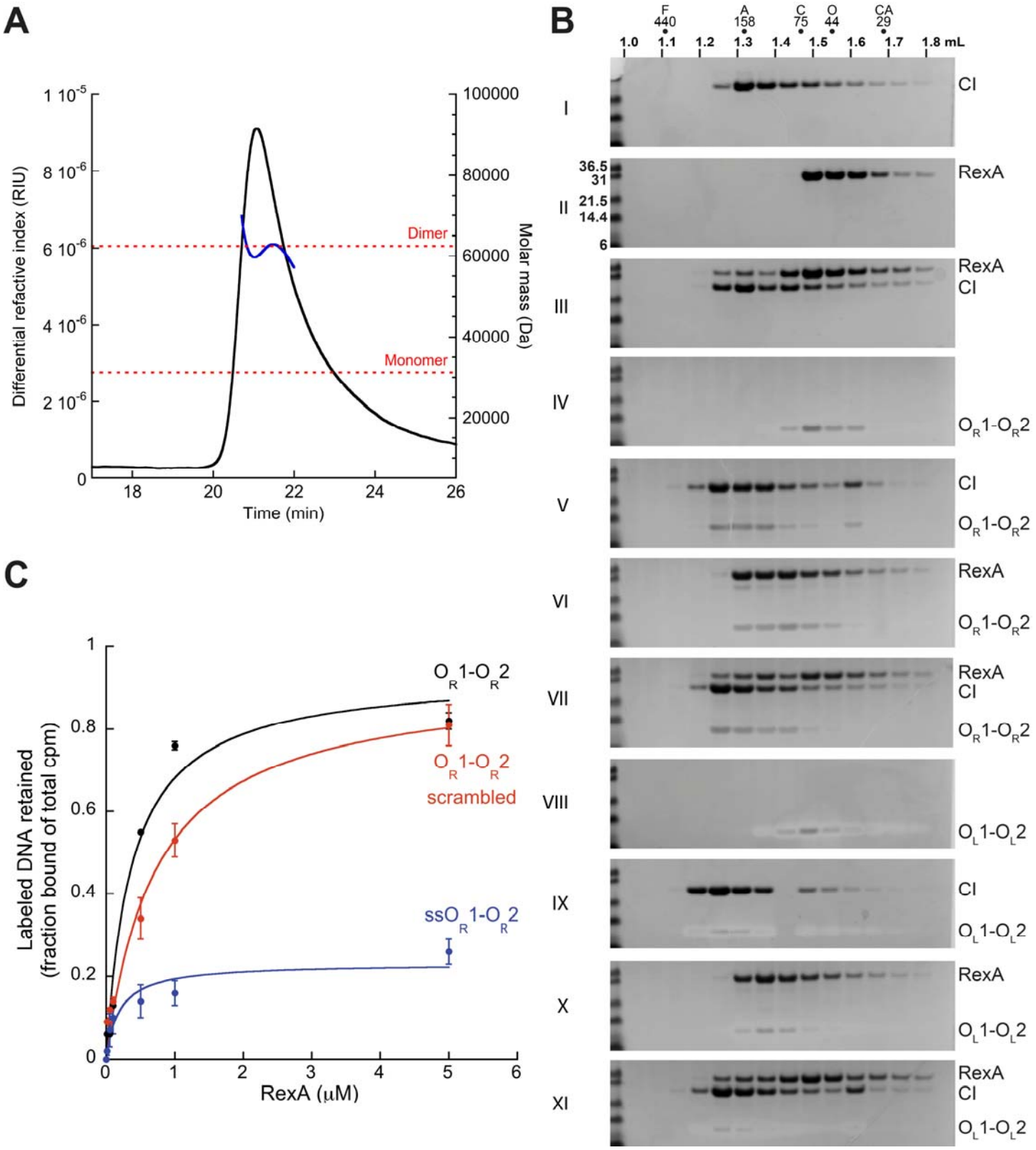

Figure 9

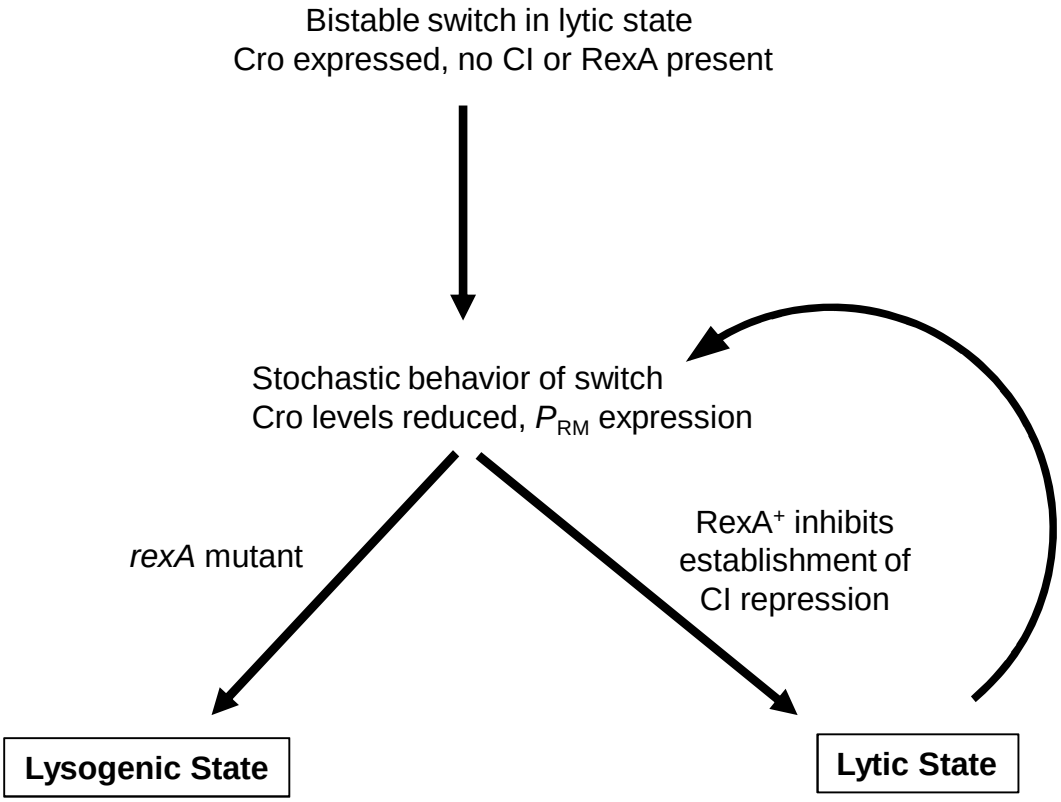

Figure 10

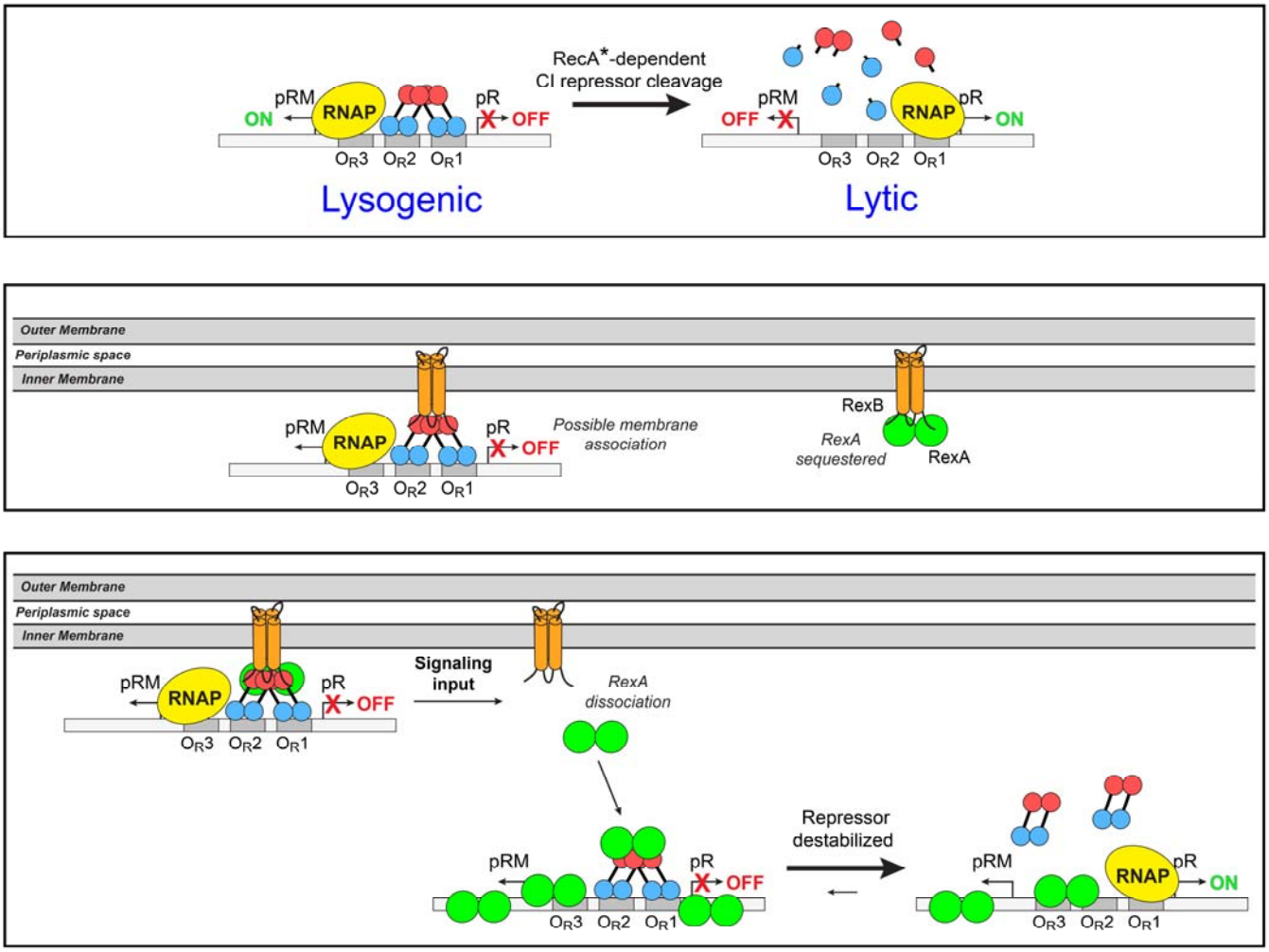

Figure 11